Frekvencijske karakteristike elektronskih kola

Prenosne funkcije (nule i polovi)

Amplitudno-frekvencijski i

fazno-frekvencijski dijagrami

Frekvencijski nezavisno kolo
Pojacanje A ne zavisi od f

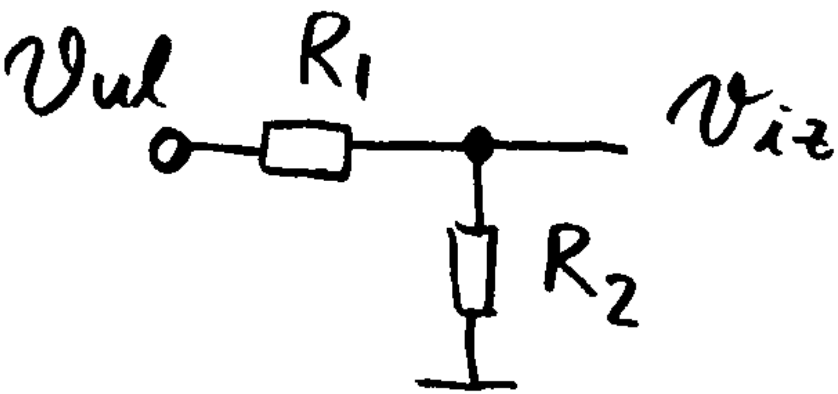

$$V_{iz} = \frac{R_2}{R_1 + R_2} V_{ul}$$

$$A = \frac{V_{iz}}{V_{ul}} = \frac{R_2}{R_1 + R_2}$$

Frekvencijski zavisno kolo primjer 1.

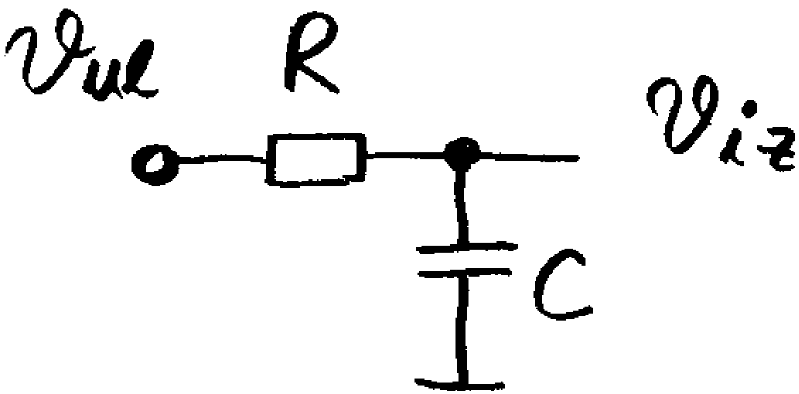

$$A = \frac{V_{iz}(s)}{V_{ul}(s)} = \frac{\frac{1}{sC}}{R + \frac{1}{sC}}$$

$$A = \frac{1}{1 + sCR}$$

$$s_p = -\frac{1}{CR}$$

Ucestanost (frekvencija) s
Nulta ucestanost s=0
Realna ucestanost s=jw

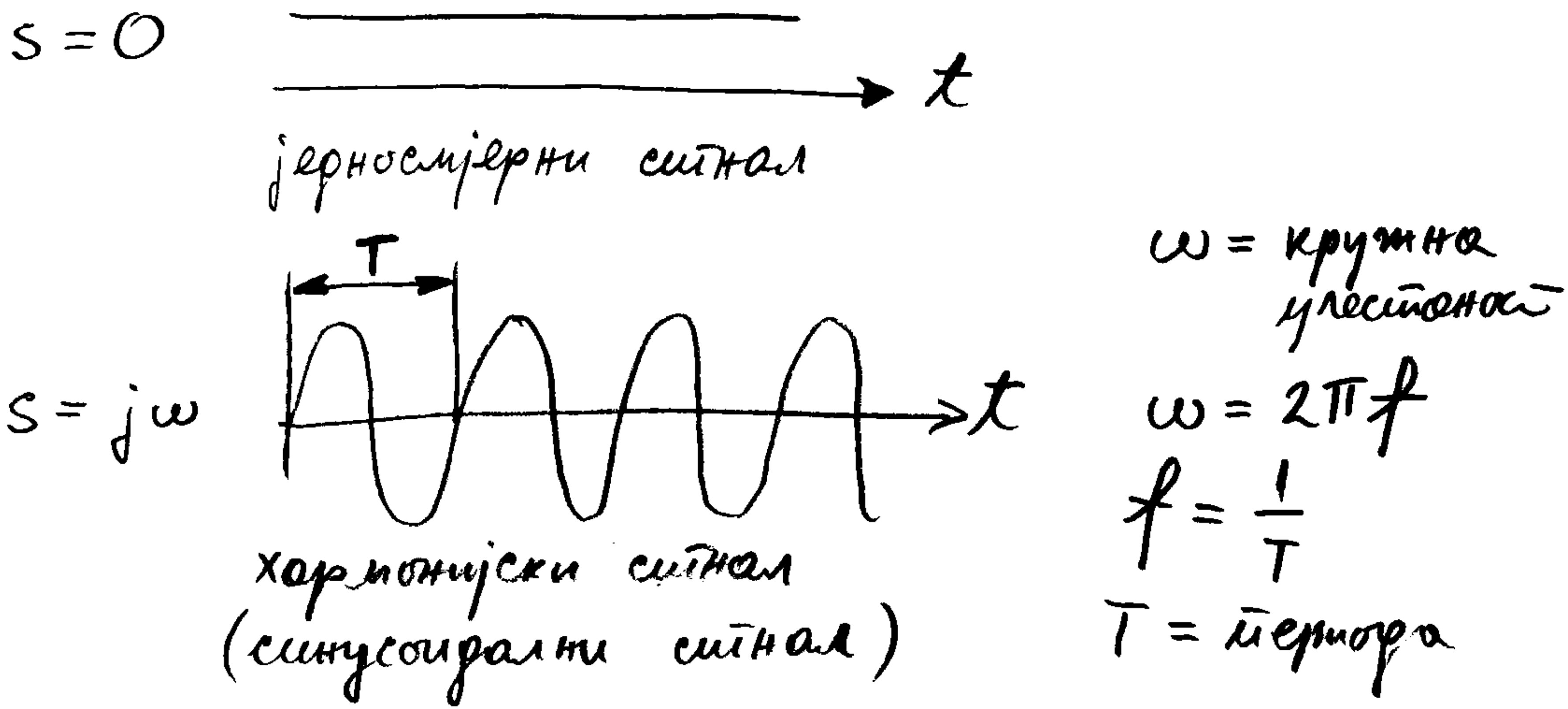

Imaginarna ucestanost

Kompleksna ucestanost

$s = \sigma + j\omega$

$\sigma > 0$

експоненцијално растући хармонијски сигнал

ω = реална учестаност

σ = имагинарна учестаност

Kada u A(s) stavimo s=jw, dobijamo prenosnu funkciju za realne ucestanosti A(jw)

Kompleksno pojacanje A(jw)

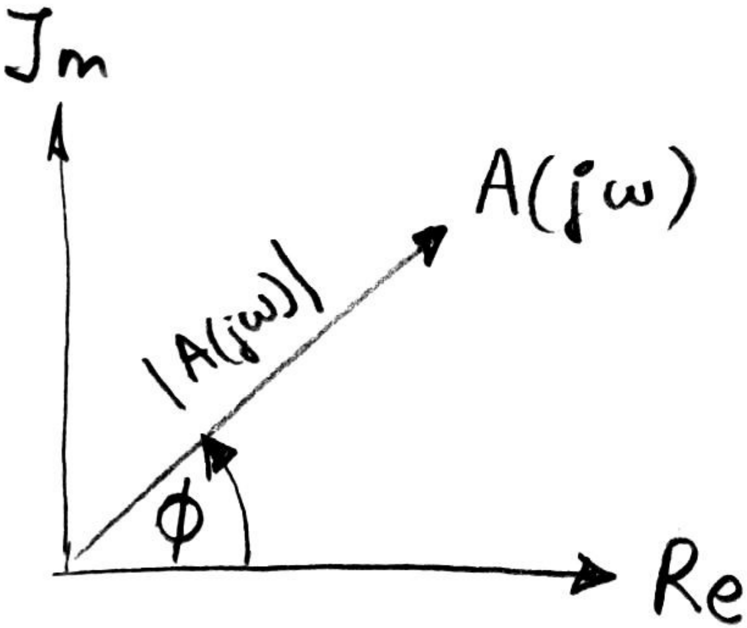

$$\Phi = Arg\{A(j\omega)\}$$

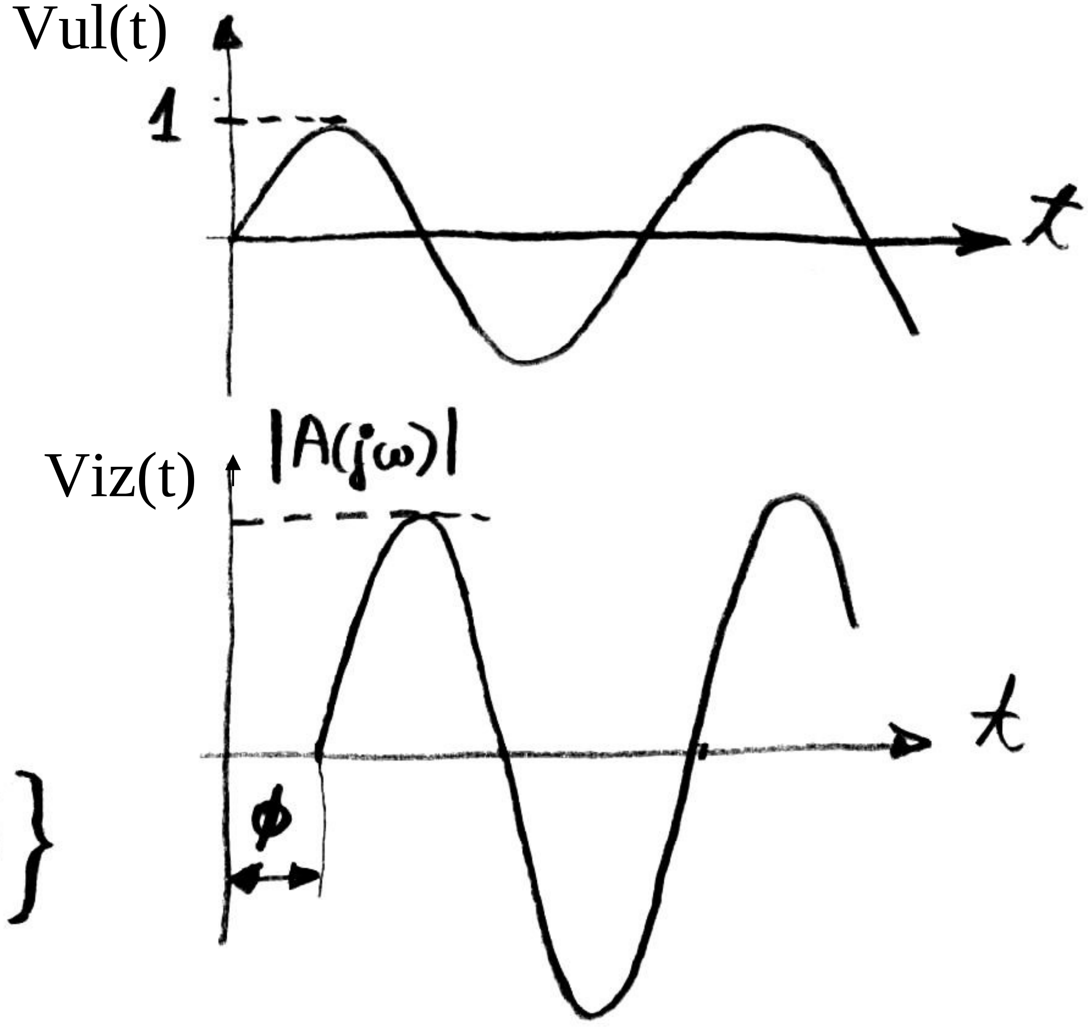

Moduo pojacanja - primjer 1

$$|A(j\omega)| = \left| \frac{1}{1 + j\omega CR} \right| = \frac{1}{\sqrt{1 + \omega^2 C^2 R^2}}$$

$$A_{dB} = 20 \log |A(j\omega)| = 20 \log \frac{1}{\sqrt{1 + \omega^2 C^2 R^2}}$$

$$A_{dB} = 20 (-1) \frac{1}{2} \log (1 + \omega^2 C^2 R^2)$$

Asimptote AdB linearna f(logw)

$\omega \to 0 \qquad AdB \to -10 \log 1 = 0$

$\omega CR \gg 1 \qquad AdB = -10 \log(\omega^2 C^2 R^2) = -20 \log \omega CR$

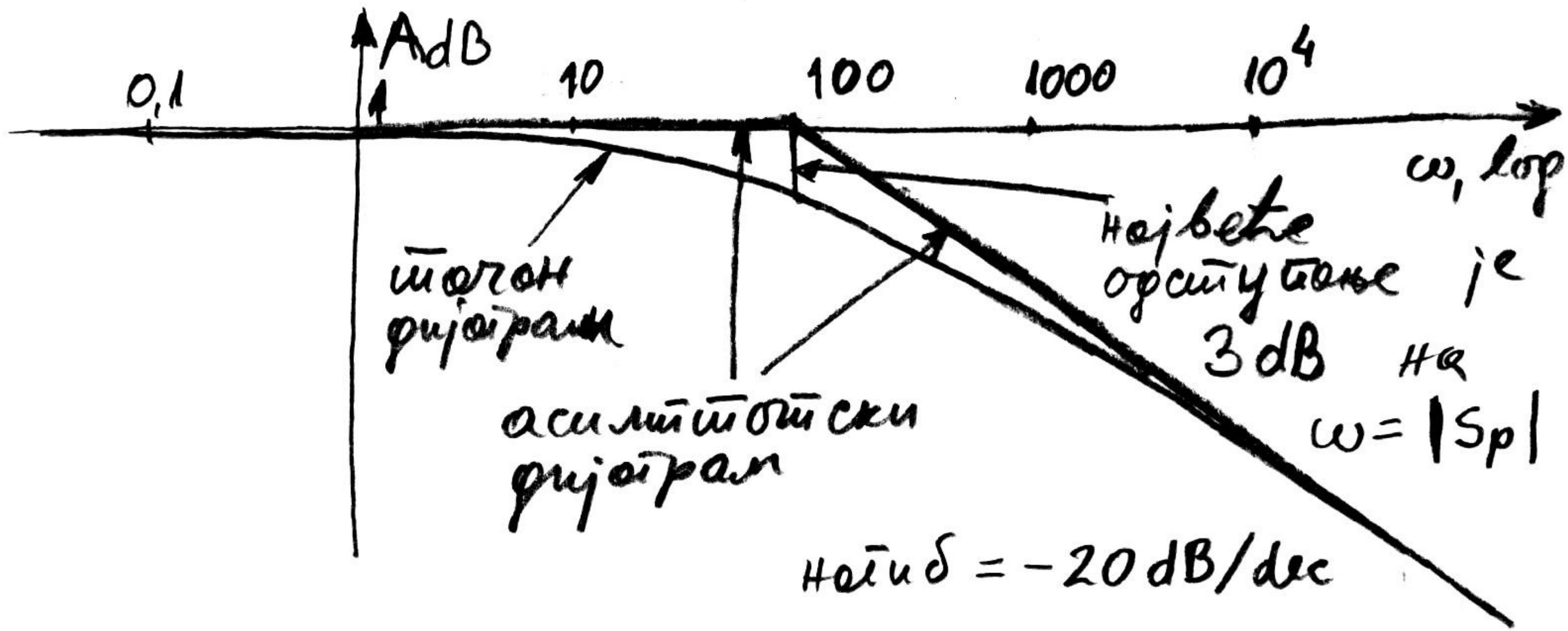

Logaritamsko pojacanje AdB

- A= 0.001 AdB= -60dB
- A=0.01 AdB= -40dB
- A=0.1 AdB= -20dB
- A=1/2 AdB= -6dB
- A=1 AdB= 0dB
- A=2 AdB= +6dB
- A=10 AdB= +20dB
- A=100 AdB= +40dB

Faza prenosne funkcije - primjer 1

$$A(j\omega) = \frac{1}{1 + j\omega CR}$$

$$\Phi(j\omega) = \text{Arg}\{A(j\omega)\} = \text{arctg}\,\frac{\text{Im}\{A(j\omega)\}}{\text{Re}\{A(j\omega)\}} = -\text{arctg}\,\frac{\omega RC}{1}$$

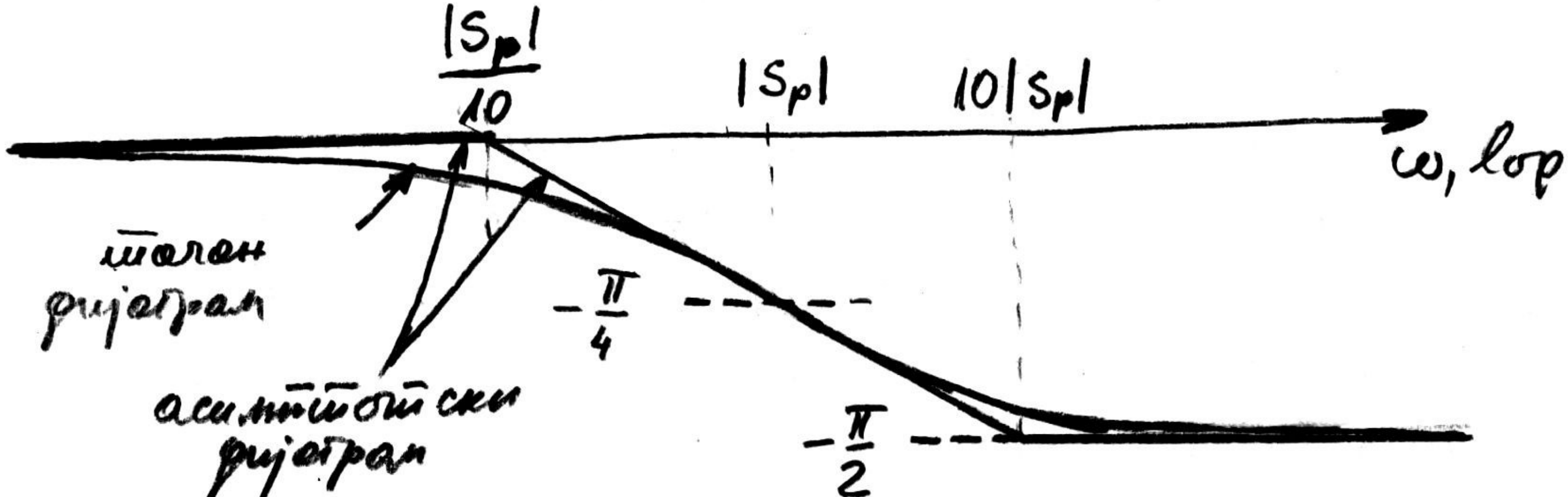

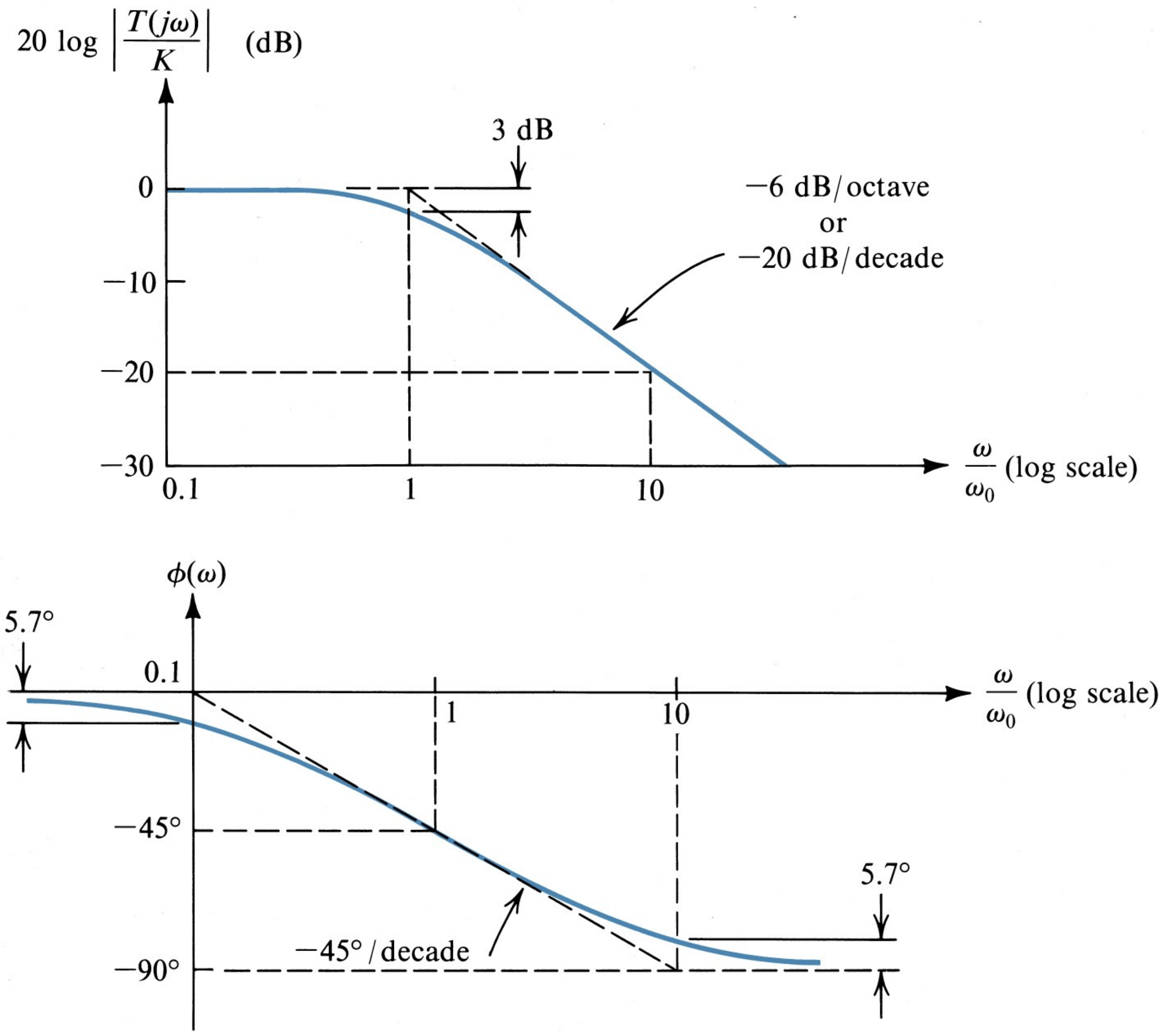

Fig. 1.23 **(a)** Magnitude and **(b)** phase response of STC networks of the low-pass type.

Prenosna funkcija sa nulom

$$A(s) = 1 + sRC \qquad s_n = -\frac{1}{RC}$$

$$|A(j\omega)| = \sqrt{1+\omega^2R^2C^2}$$

$$A_{dB} = 20\log|A(j\omega)| = +10\log(1+\omega^2R^2C^2)$$

$$\Phi = \operatorname{Arg}\{A(j\omega)\} = \operatorname{arctg}\omega RC$$

Amplitudski i fazni dijagram prenosne funkcije sa nulom

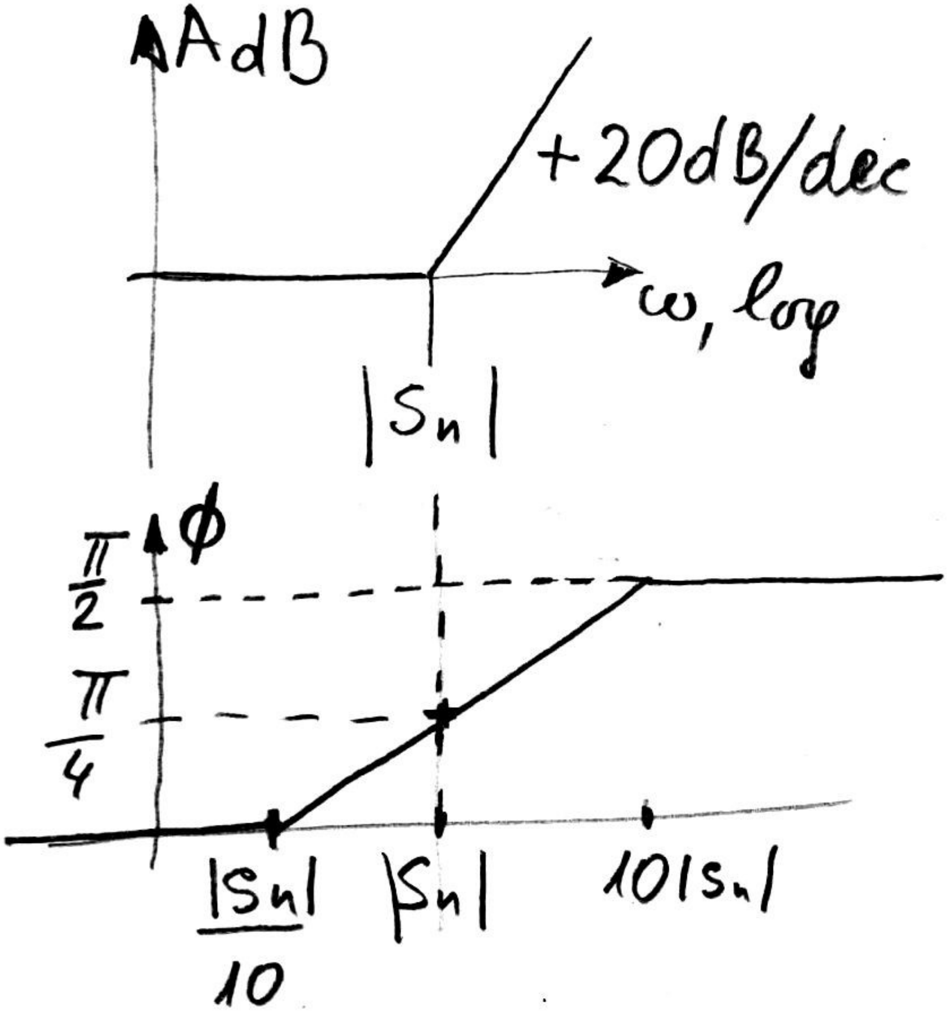

Нула повећава нагиб AdB за 20dB/dec

Нула подиже фазну карактеристику за $\frac{\pi}{2}$.

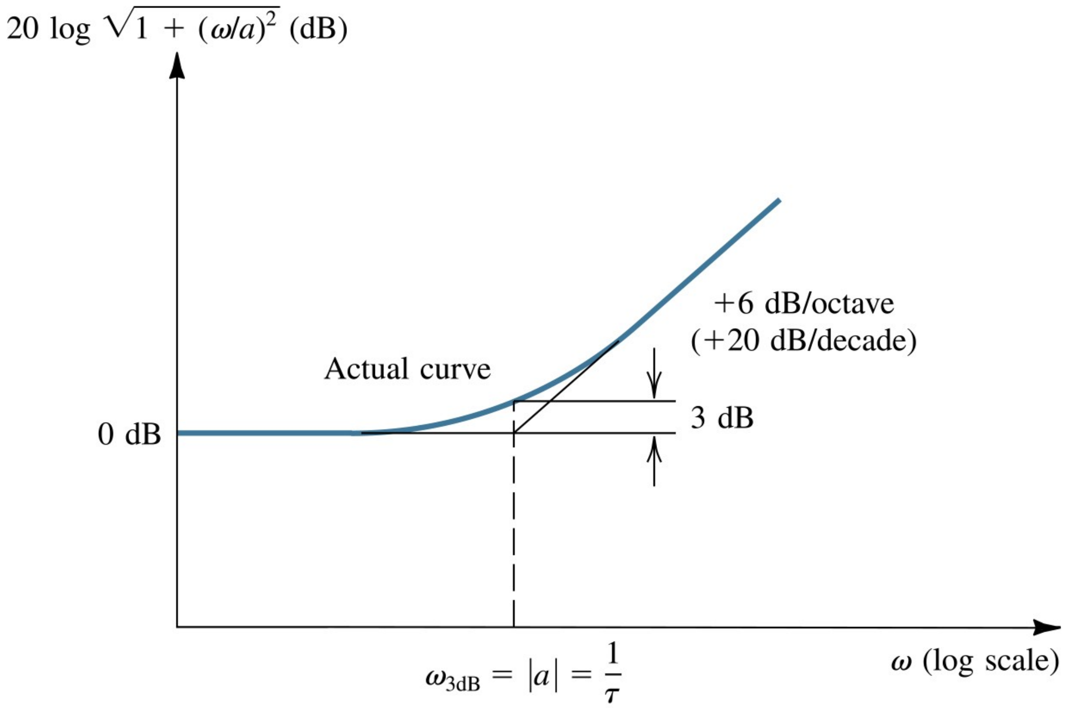

Fig. 7.1 Bode plot for the typical magnitude term. The curve shown applies for the case of a zero. For a pole, the high-frequency asymptote should be drawn with a −6-dB/octave slope.

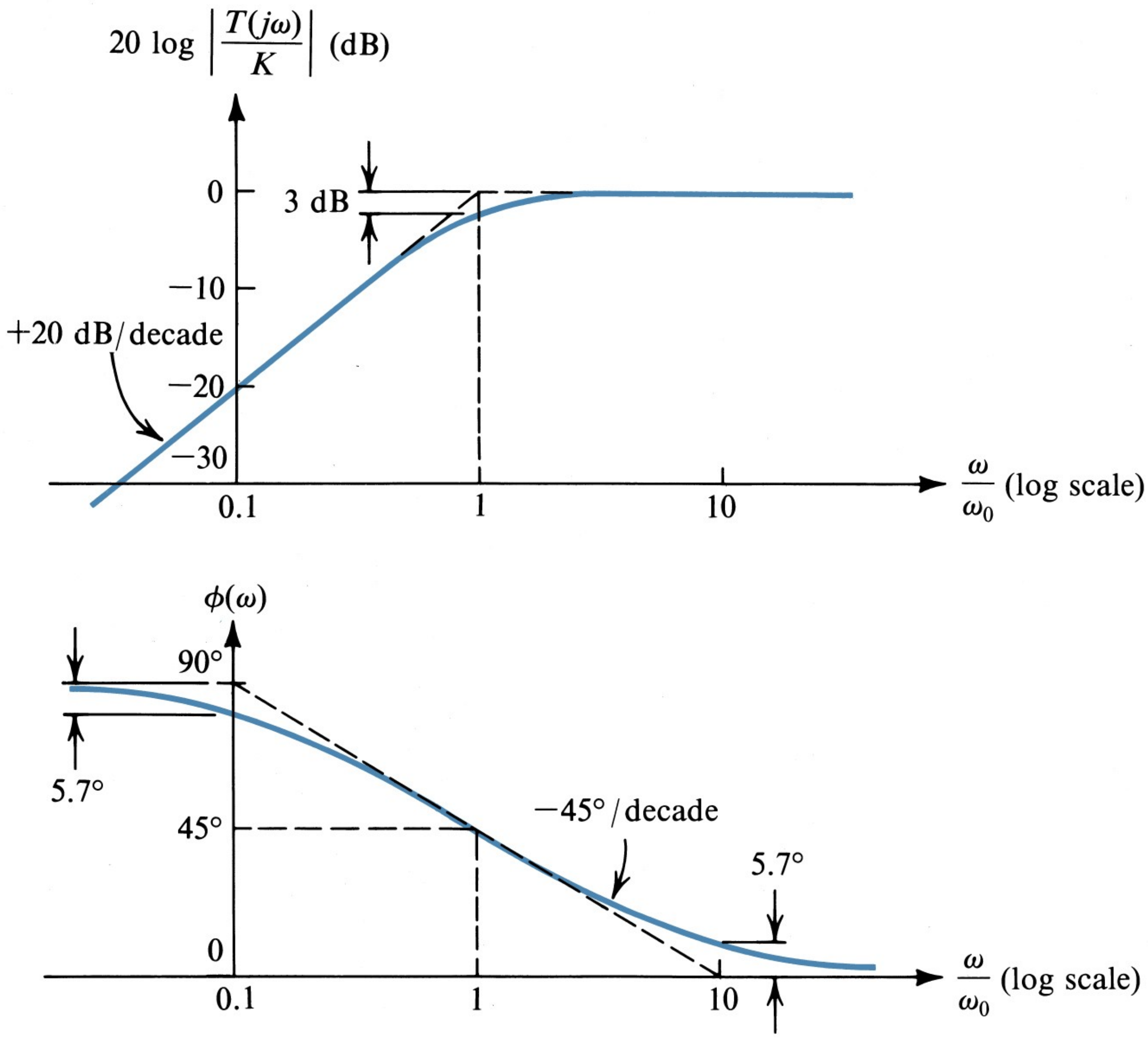

Fig. 1.24 (a) Magnitude and **(b)** phase response of STC networks of the high-pass type.

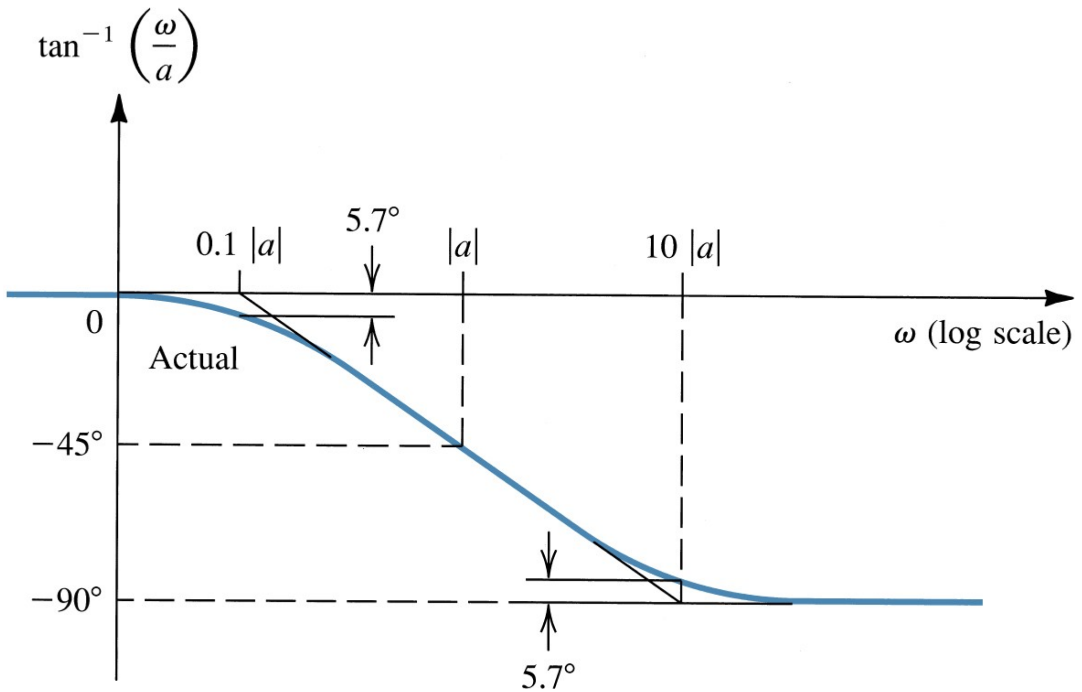

Fig. 7.3 Bode plot of the typical phase term $\tan^{-1}(\omega/a)$ when a is negative.

U opstem slucaju kolo ima vise nula i polova

$$A(j\omega) = K \frac{(s - s_{n1})(s - s_{n2})\dots}{(s - s_{p1})(s - s_{p2})\dots}$$

$$A_{dB} = 20\log K + 20\log|j\omega - s_{n1}| + 20\log|j\omega - s_{n2}| + \dots$$

$$- 20\log|j\omega - s_{p1}| - 20\log|j\omega - s_{p2}| - \dots$$

$$\phi = \text{Arg}\{j\omega - s_{n1}\} + \text{Arg}\{j\omega - s_{n2}\} + \dots$$

$$- \text{Arg}\{j\omega - s_{p1}\} - \text{Arg}\{j\omega - s_{p2}\} - \dots$$

Uticaj nula na AFK i FFK

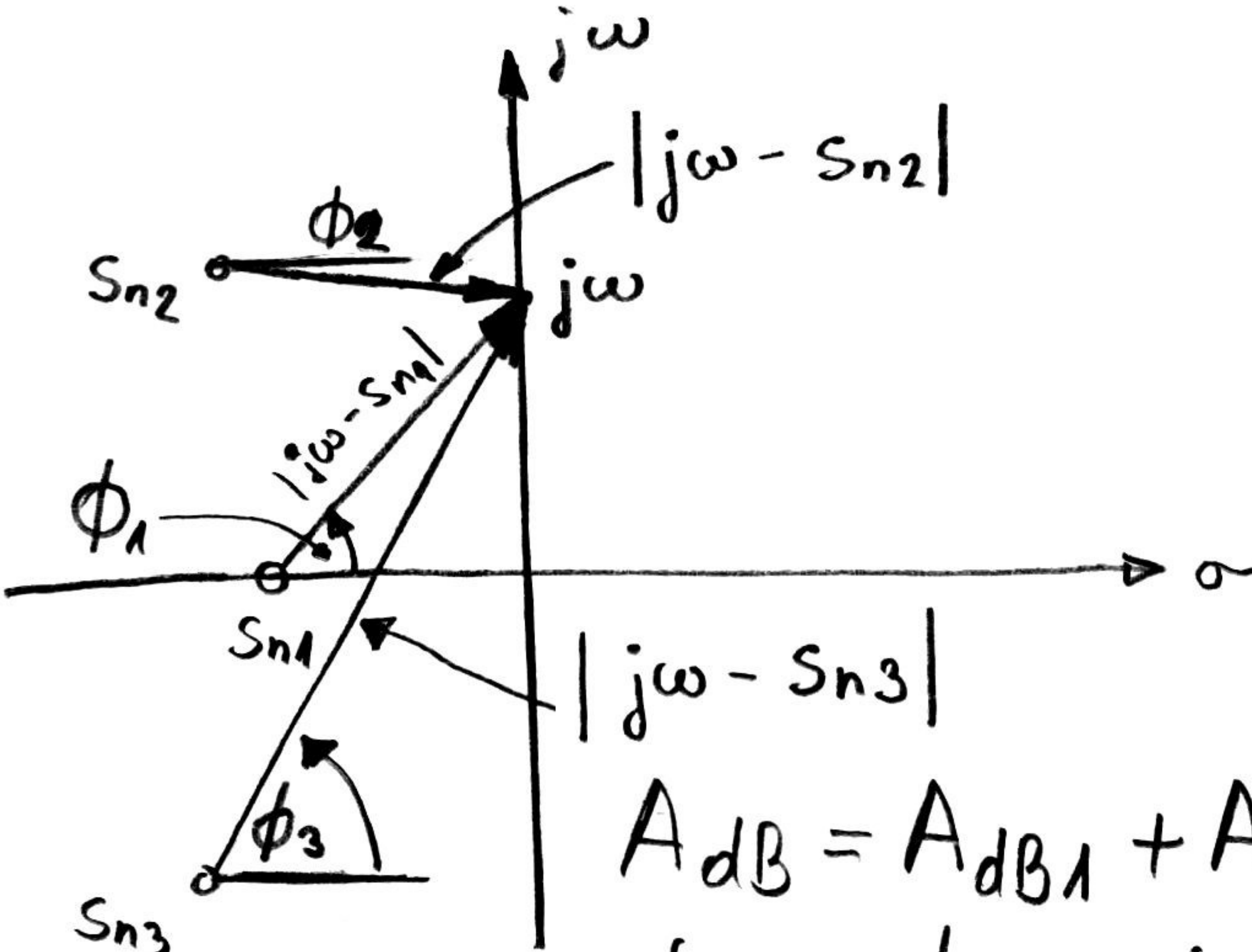

$$A_{dB} = A_{dB1} + A_{dB2} + A_{dB3}$$

$$\phi = \phi_1 + \phi_2 + \phi_3$$

Konjugovano kompleksni par nula blizu jw ose unosi rezonantno ulegnuce i strmiju promjenu faze

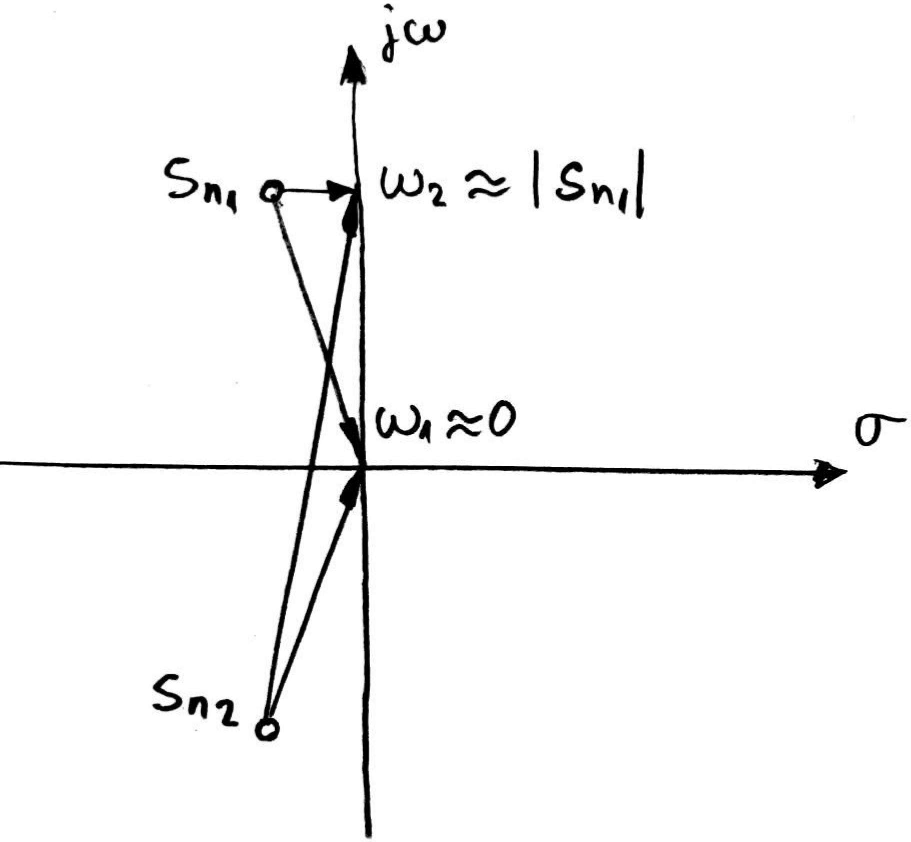

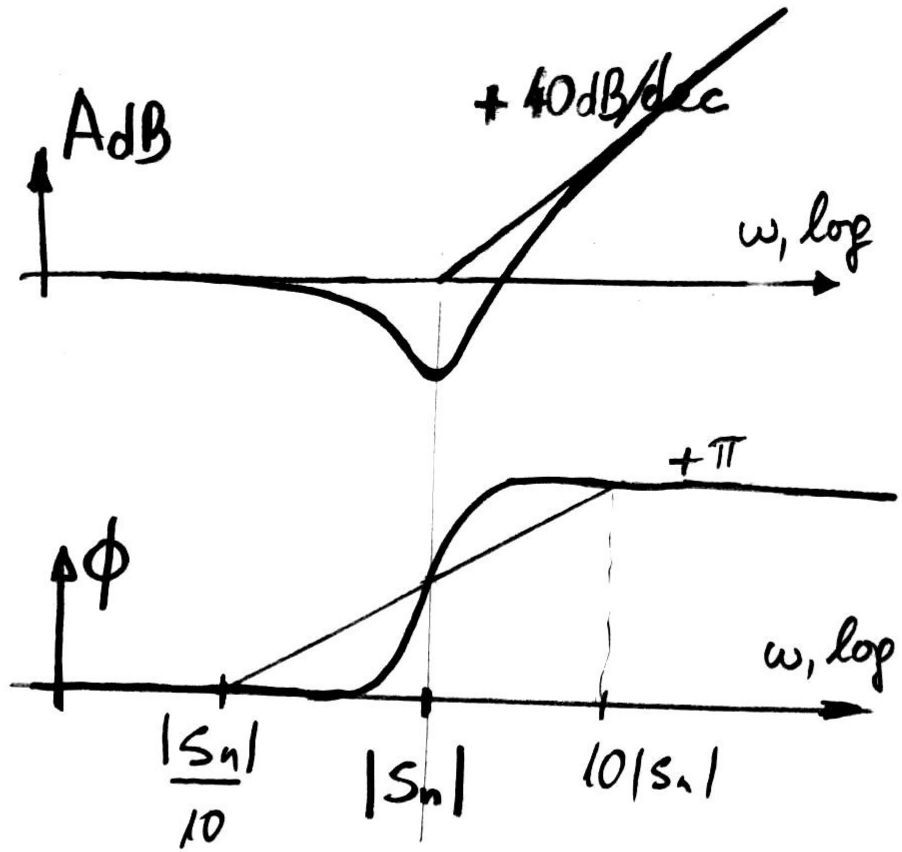

Uticaj slabo prigusenih polova na AFK i FFK

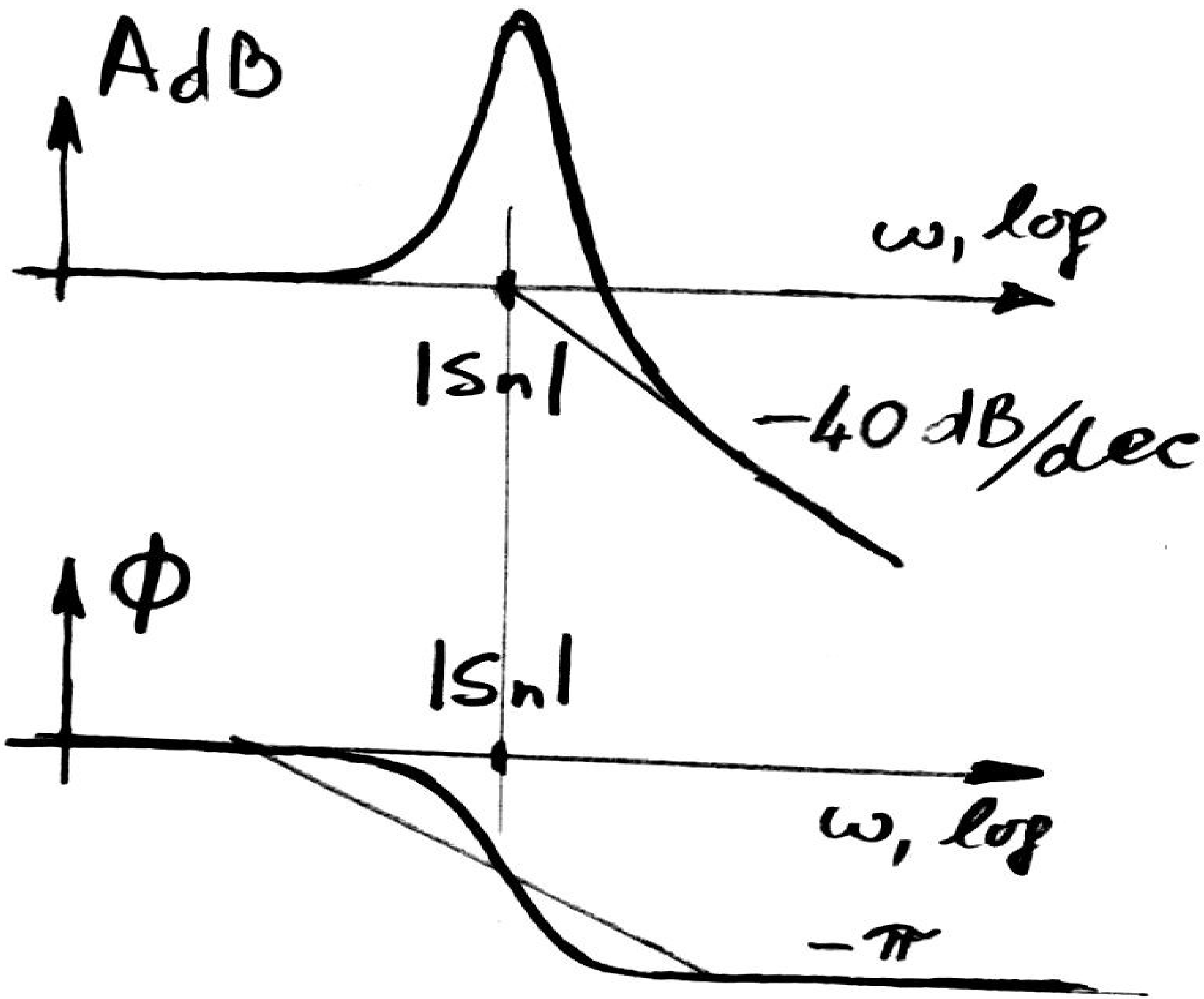

Analiza frekvencijskih karakteristika

- Nalazenje prenosne funkcije kola
- Nalazenje nula i polova ove funkcije
- Crtanje AF i FF dijagrama

Nalazenje prenosne funkcije kola

- Elektronske komponente (tranzistore, diode, itd) zamjenimo modelima za male signale i svodimo problem na linearno kolo sa koncentrisanim parametrima.
- Reaktanse uvijek donose polove.

- Kondenzator u direktnoj grani donosi nulu.

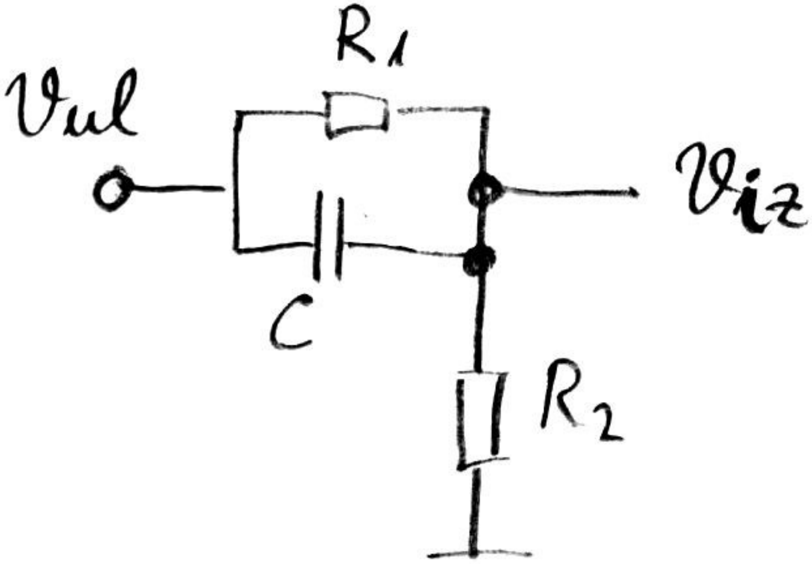

$$\omega = 0 \Rightarrow A = \frac{R_2}{R_1 + R_2}$$

$$\omega \to \infty \Rightarrow A = 1$$

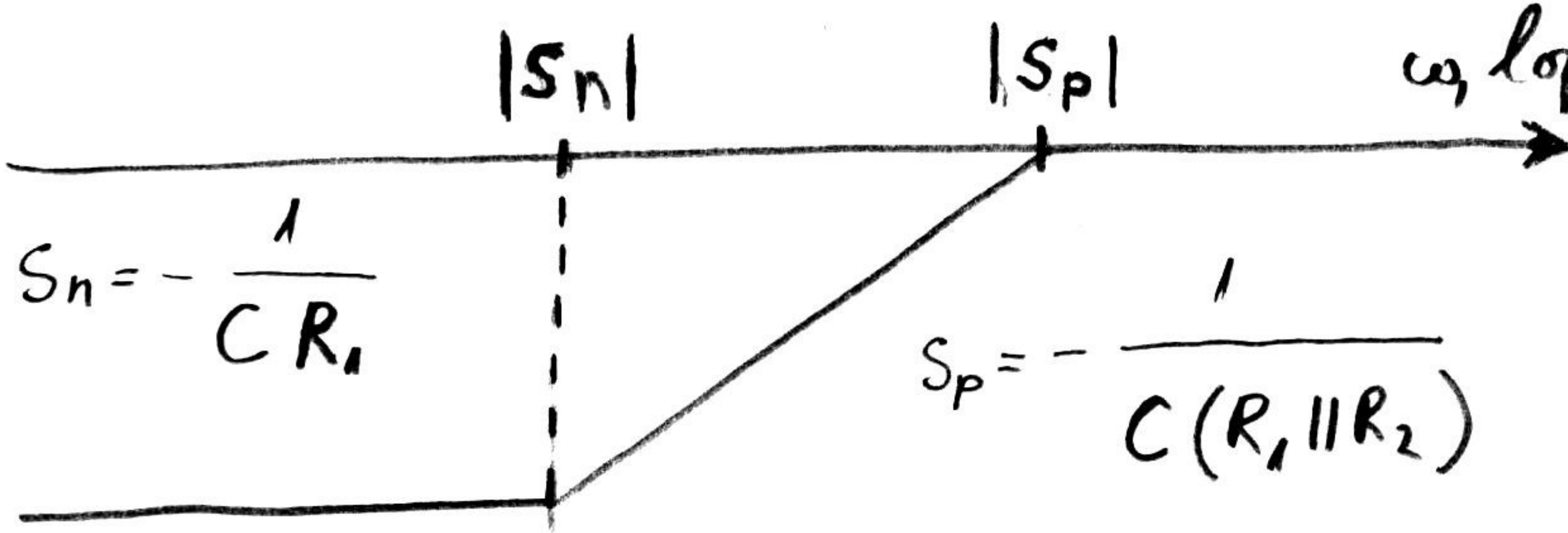

- Kondenzator u otocnoj grani donosi nulu kada je vezan na red sa otpornikom.

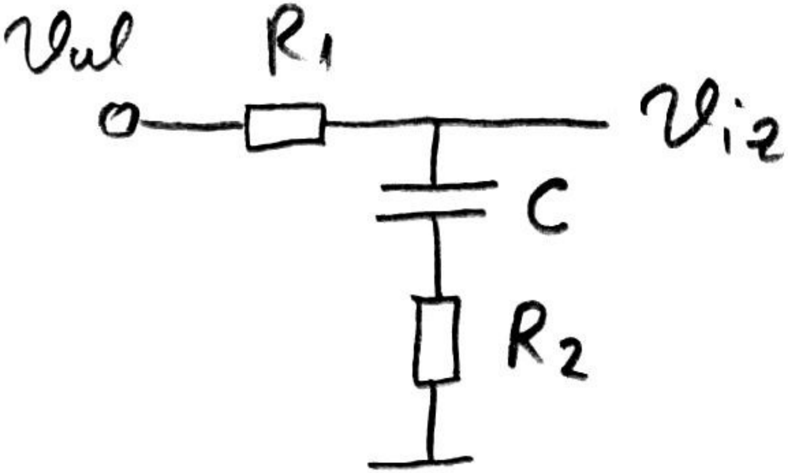

$$\omega = 0 \quad A = 1$$

$$\omega \to \infty \quad A = \frac{R_2}{R_1 + R_2}$$

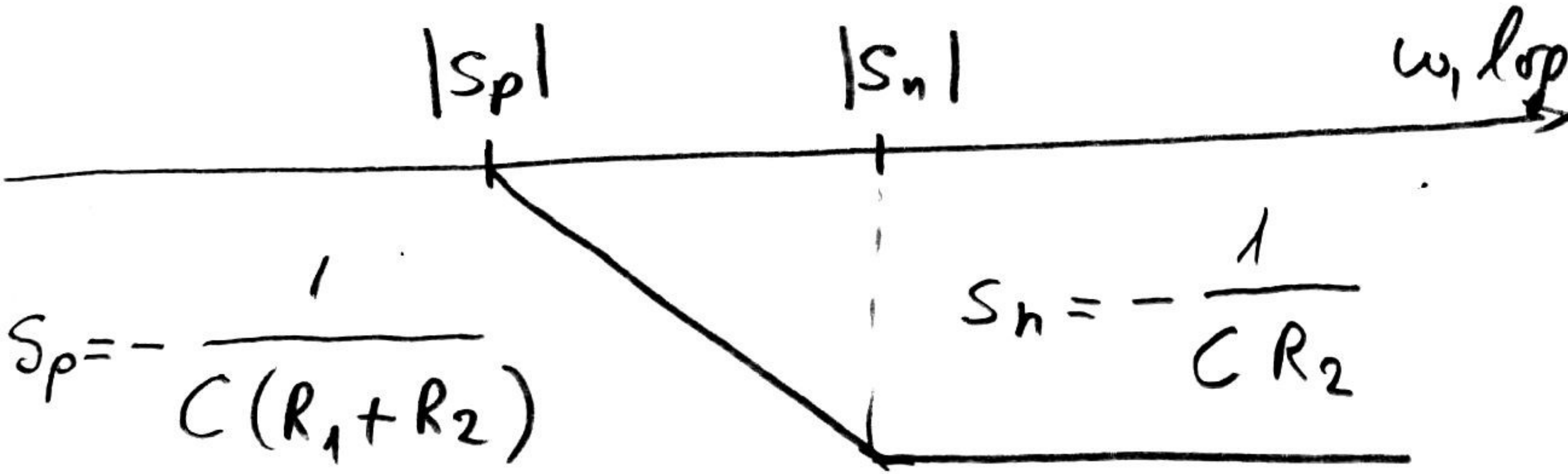

$$s_p = -\frac{1}{C(R_1 + R_2)}$$

$$s_n = -\frac{1}{C R_2}$$

- Induktivnost u otocnoj grani donosi nulu.
- Induktivnost u direktnoj grani donosi nulu kada je na red vezana sa otpornikom.
- Ucestanost pola Sp=-1/t, gdje je t=C*Re, gdje je Re ekvivalentna otpornost koju “vidi” kondenzator.
- Analogno t=L/Re, gdje je Re otpornost koju “vidi” induktivitet.

Nalazenje pola od kondenzatora

$$s_p = -\frac{1}{\tau} \qquad \tau = C \cdot R_{ek}$$

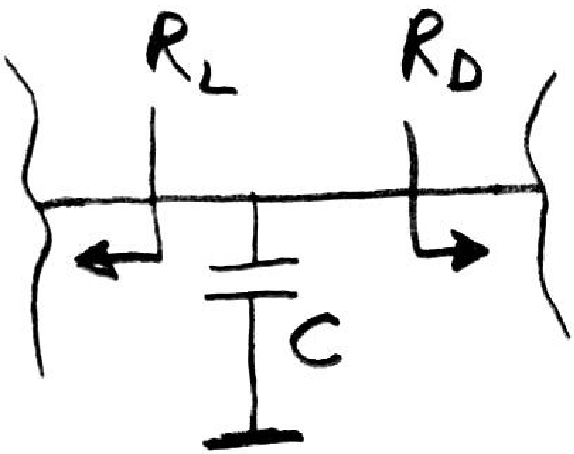

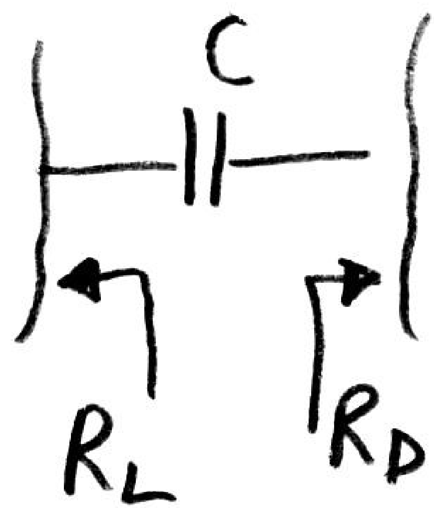

$$\tau = C \cdot (R_L \parallel R_D)$$

$$\tau = C \cdot (R_L + R_D)$$

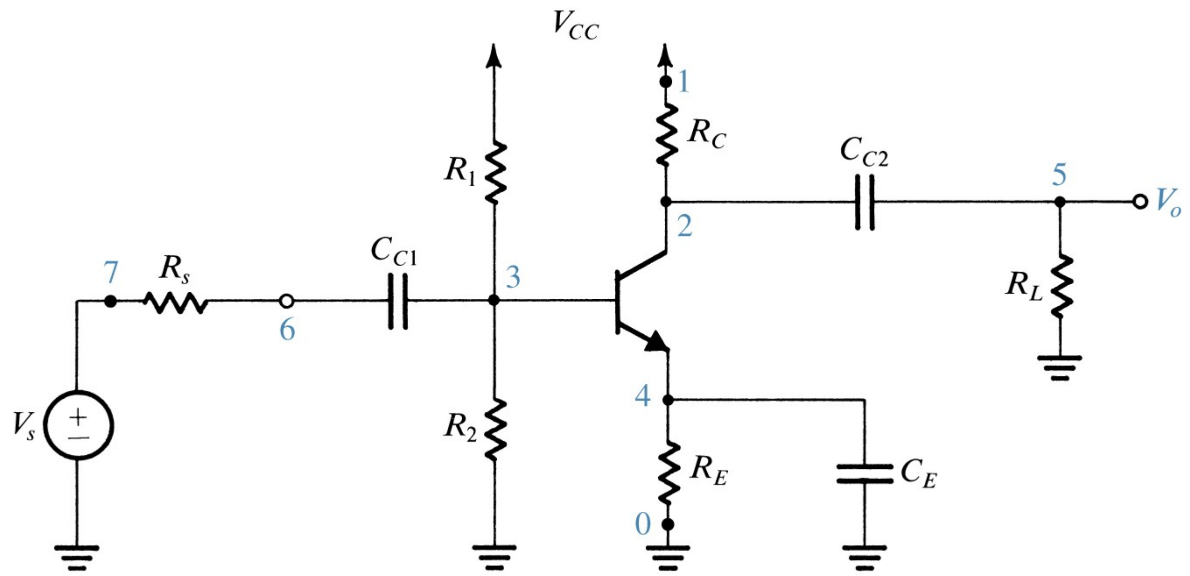

Fig. 7.13 The classical common-emitter amplifier stage. (The nodes are numbered for the purposes of the SPICE simulation in Example 7.9.)

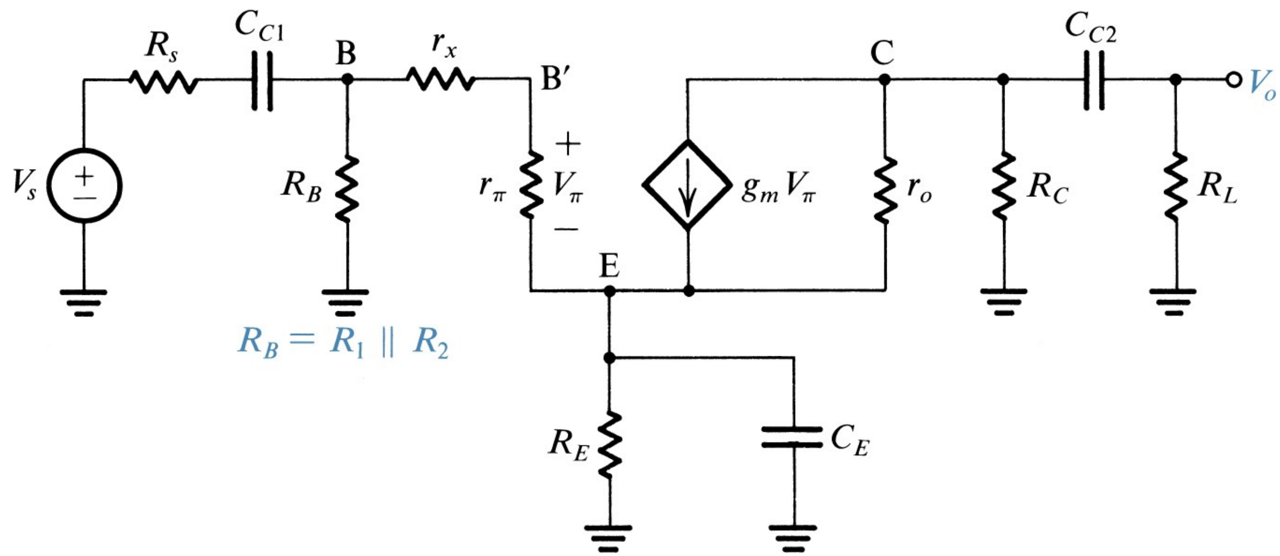

Fig. 7.14 Equivalent circuit for the amplifier of Fig. 7.13 in the low-frequency band.

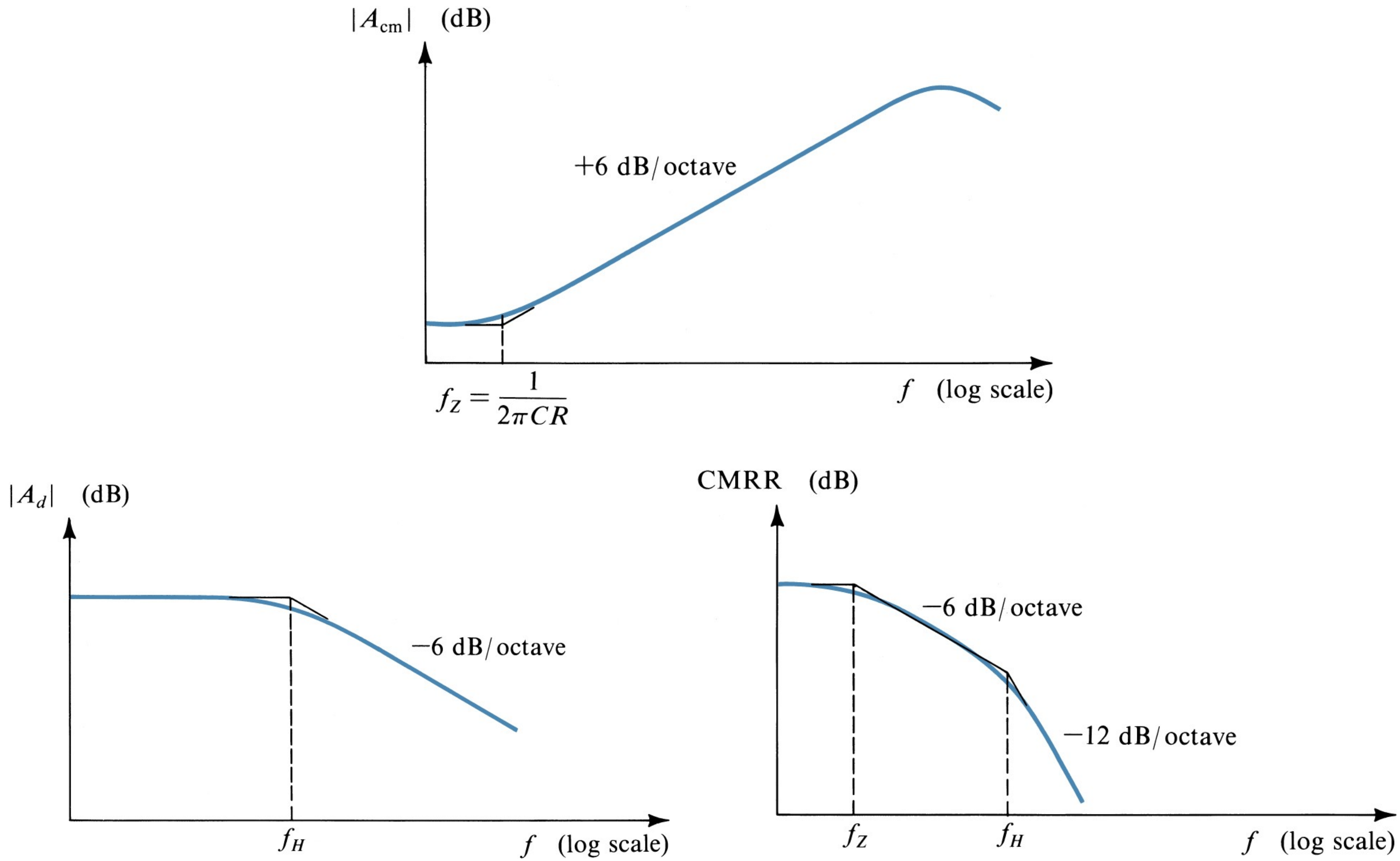

Fig. 7.33 Variation of (a) common-mode gain, (b) differential gain, and (c) common-mode rejection ratio with frequency.

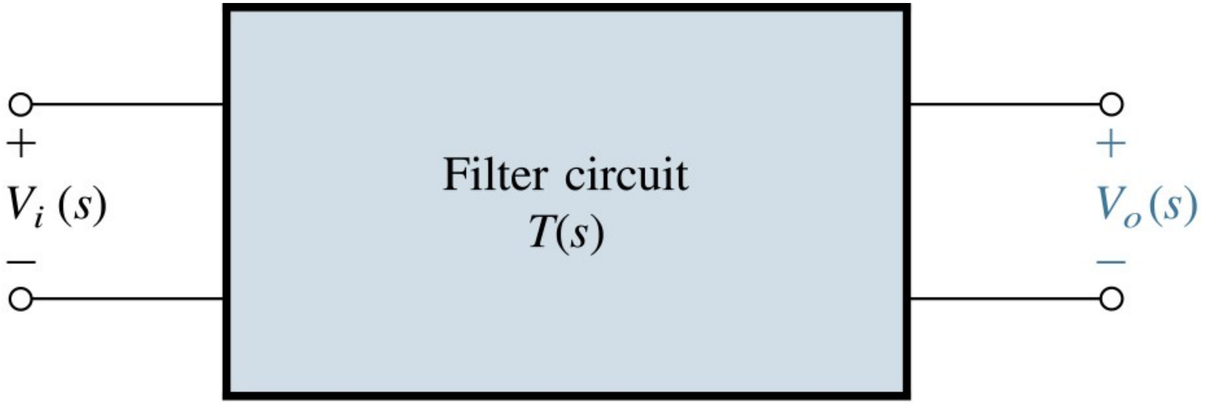

Fig. 11.1

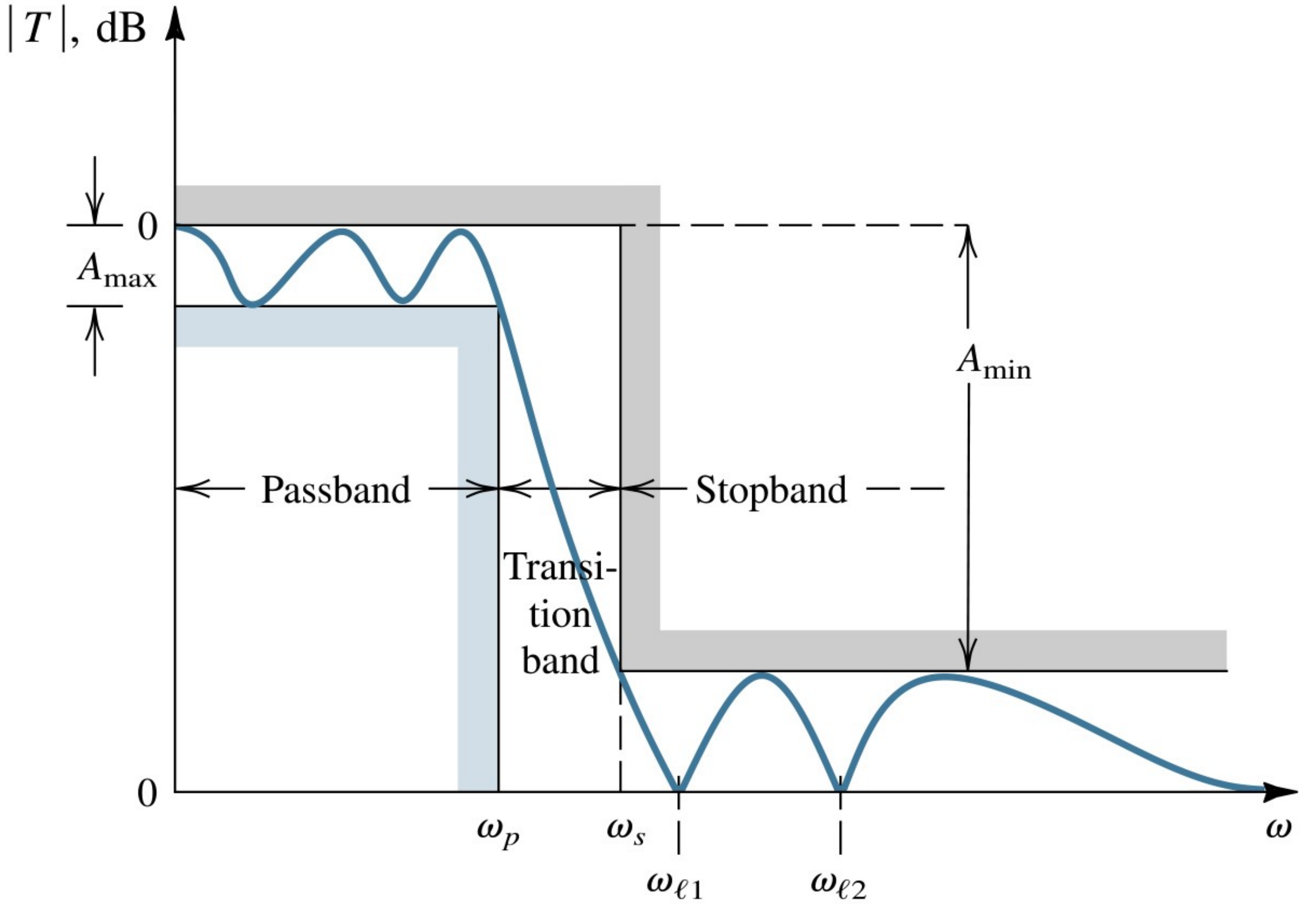

Fig. 11.3 Specification of the transmission characteristics of a low-pass filter. The magnitude response of a filter that just meets specifications is also shown.

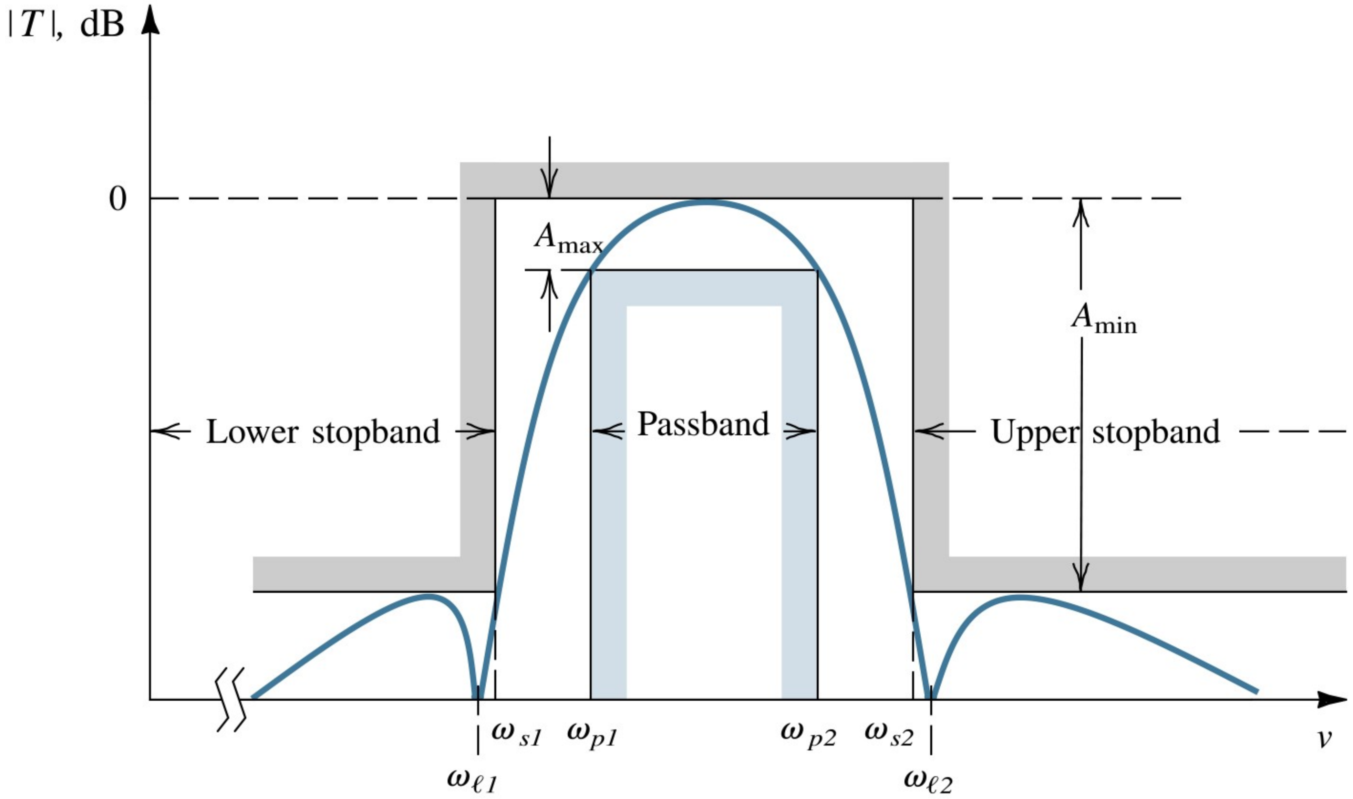

Fig. 11.4 Transmission specifications for a bandpass filter. The magnitude response of a filter that just meets specifications is also shown. Note that this particular filter has a monotonically decreasing transmission in the passband on both sides of the peak frequency.

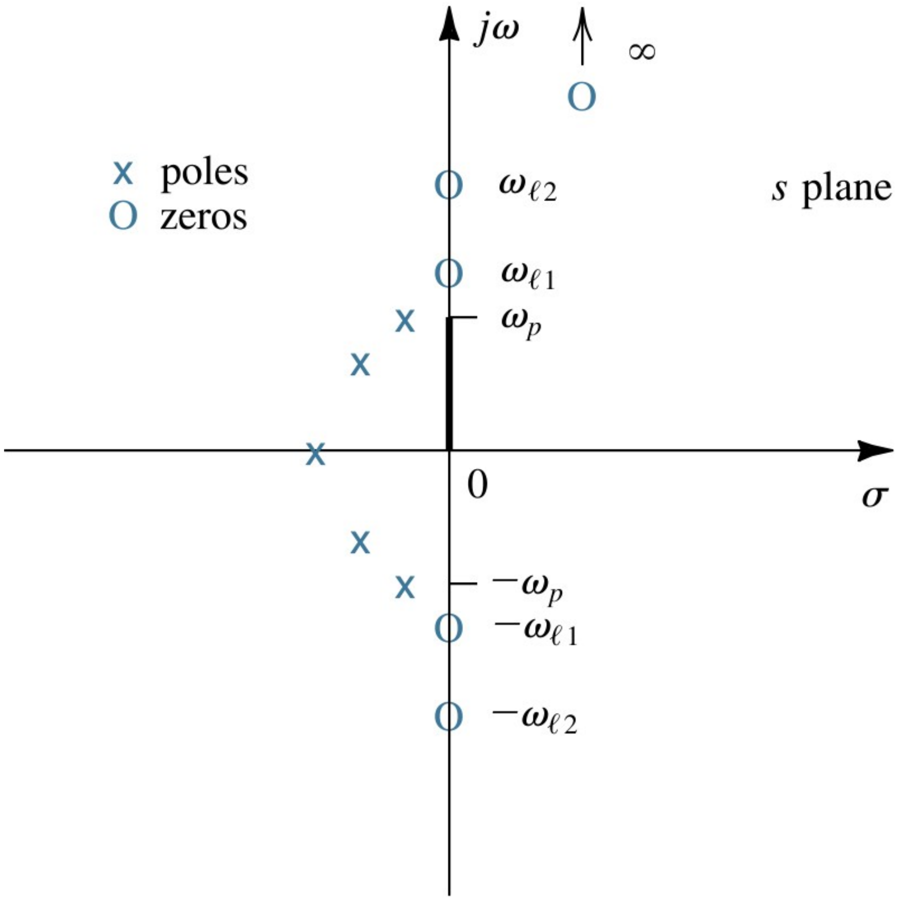

Fig. **11.5** Pole-zero pattern for the low-pass filter whose transmission is sketched in **Fig. 11.3**. This filter is of the fifth order (N = 5.)

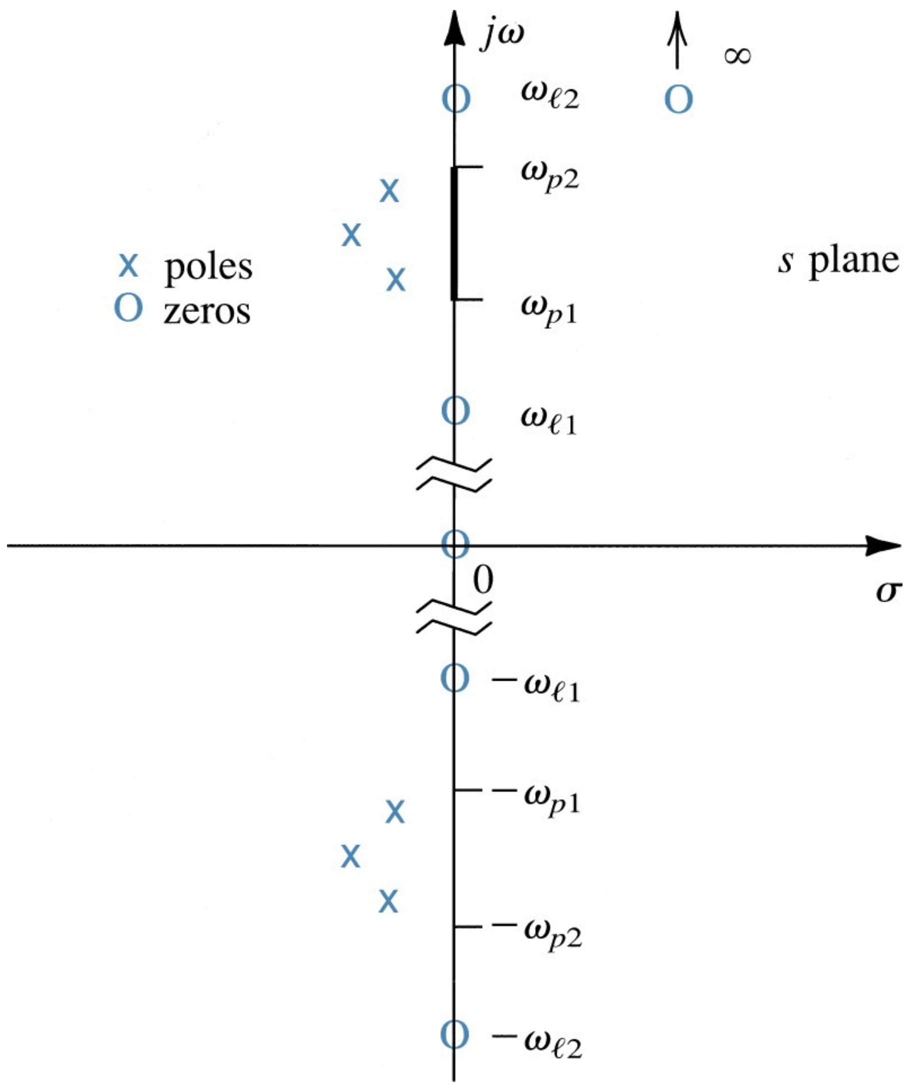

Fig. 11.6 Pole-zero pattern for the bandpass filter whose transmission is shown in **Fig. 11.4.** This filter is of the sixth order (N = 6.)

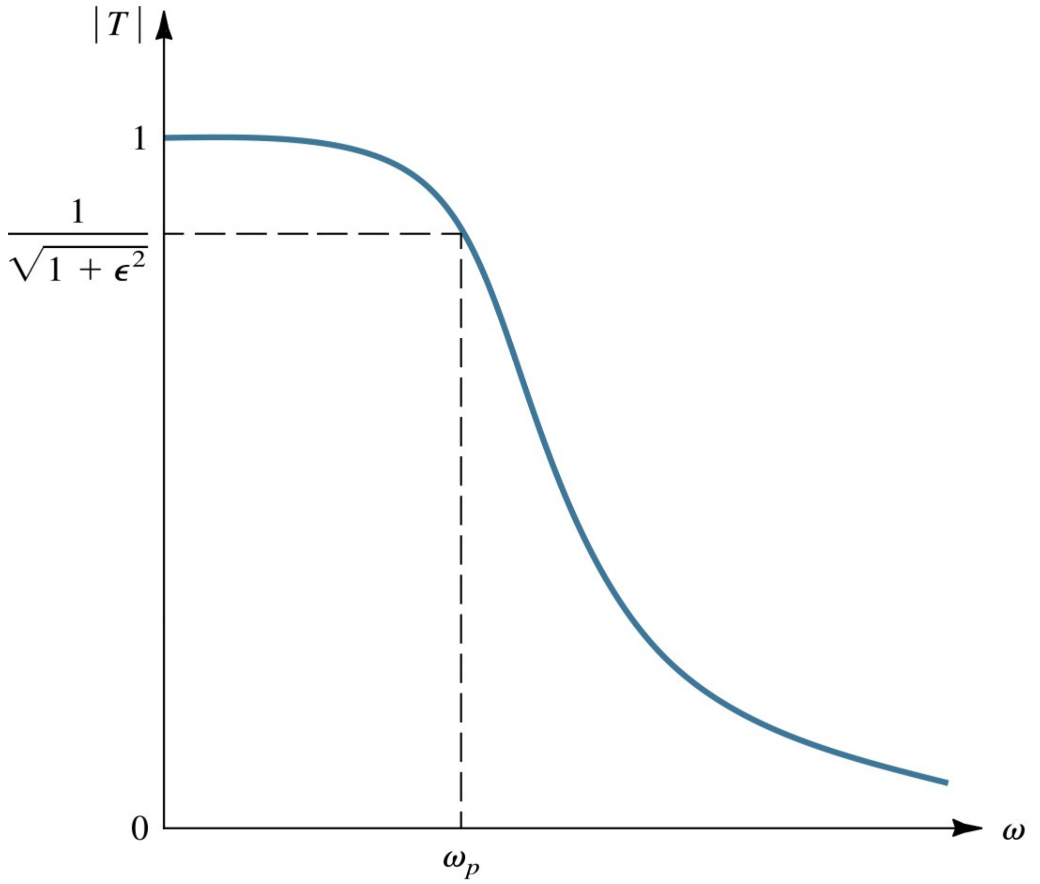

Fig. **11.8** The magnitude response of a Butterworth filter.

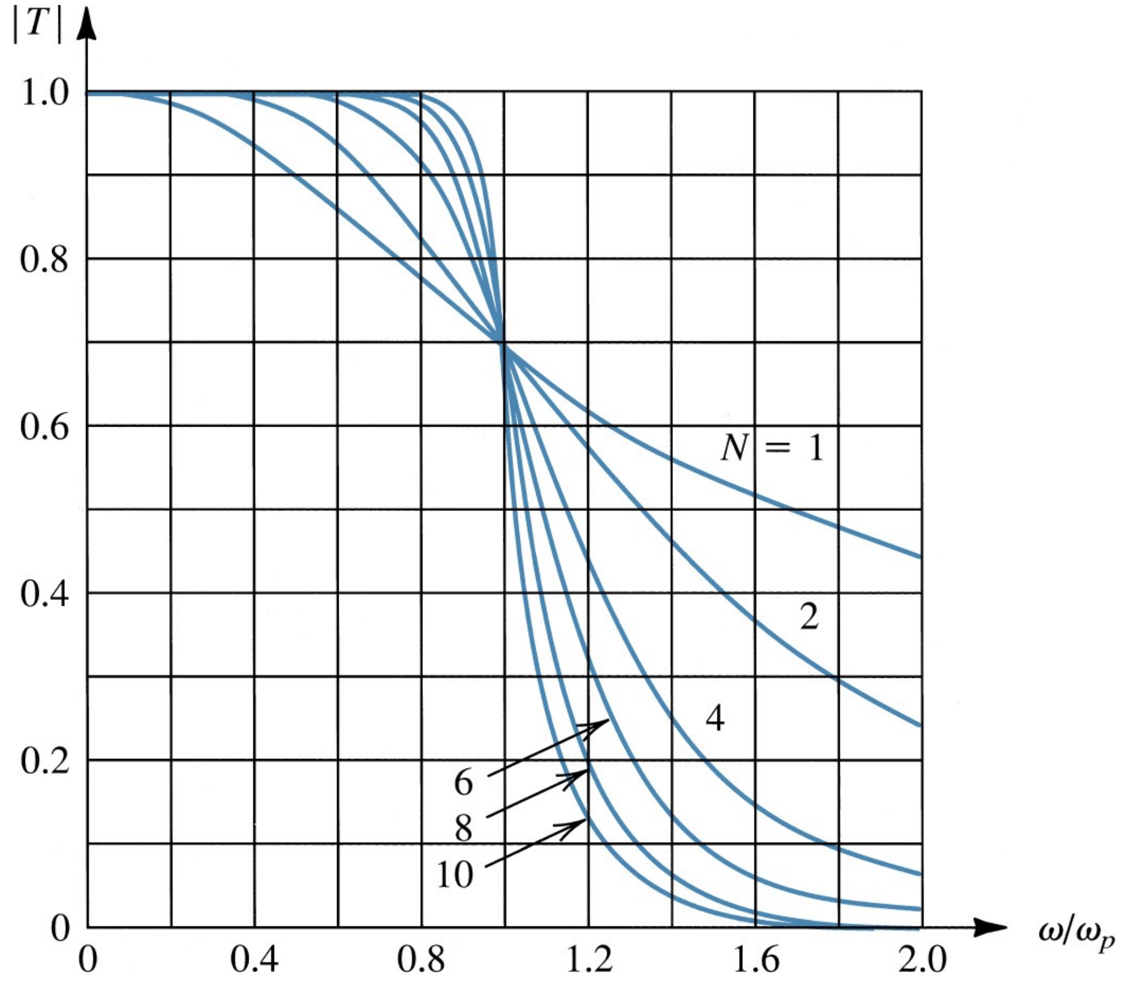

Fig. **11.9** Magnitude response for Butterworth filters of various order with ε = 1. Note that as the order increases, the response approaches the ideal brickwall type transmission.

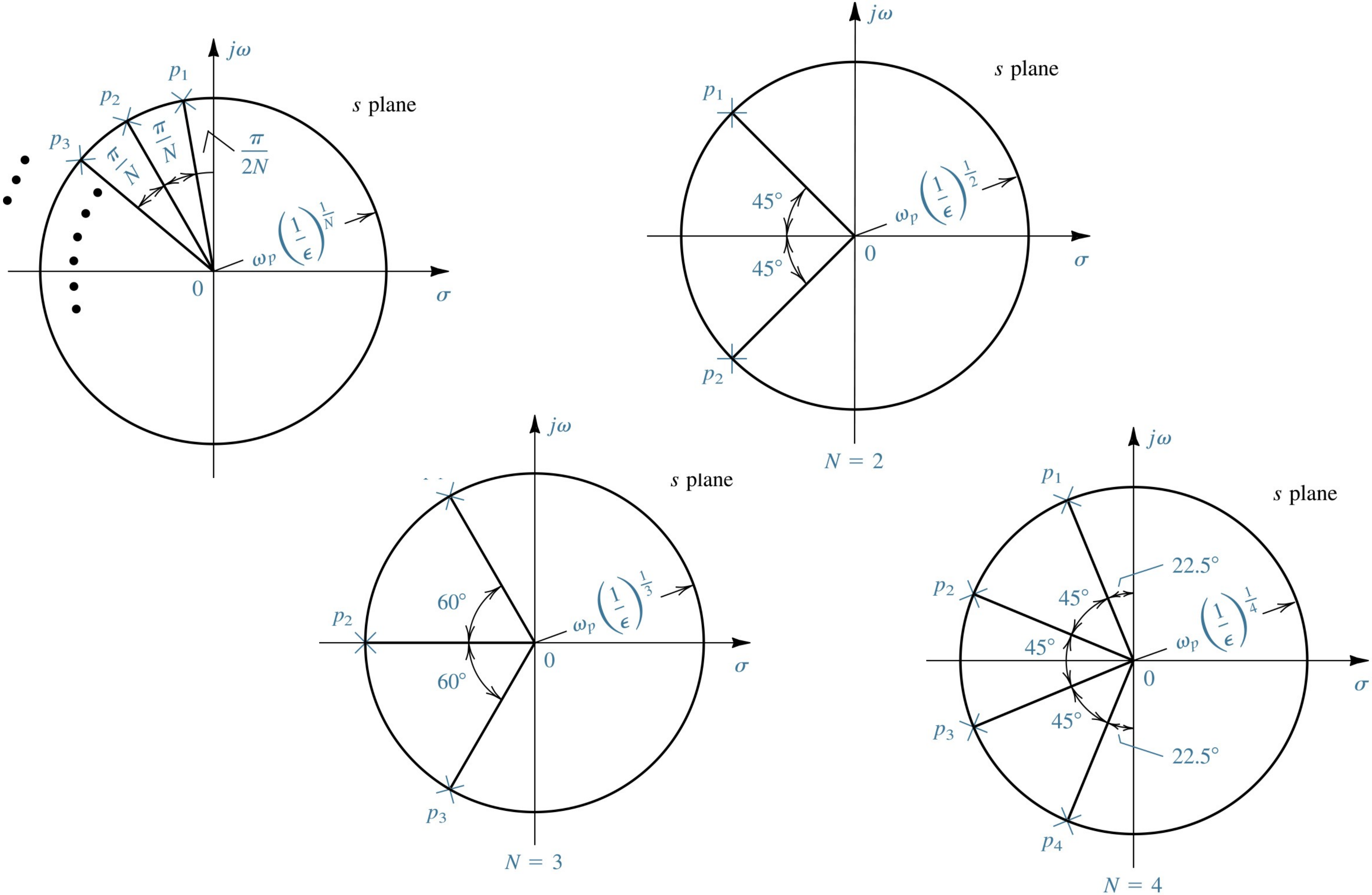

Fig. 11.10 Graphical construction for determining the poles of a Butterworth filter of order *N*. All the poles lie in the left half of the *s*-plane on a circle of radius $\omega_0 = \omega_p(1/\varepsilon)^{1/N}$, where ε is the passband deviation parameter : $\epsilon = \sqrt{10^{A_{max}/10} - 1}$

(a) the general case, **(b)** $N = 2$, **(c)** $N = 3$, **(d)** $N = 4$.

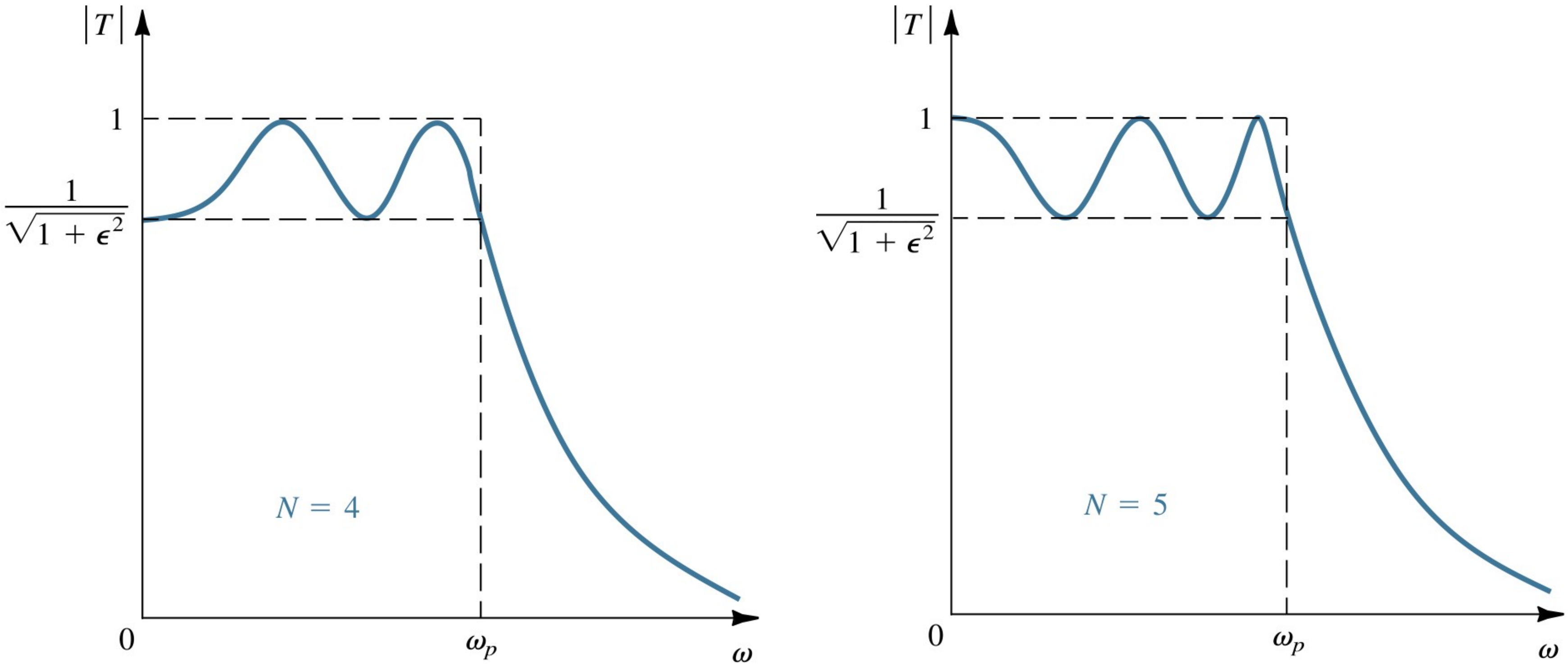

Fig. 11.12 Sketches of the transmission characteristics of a representative even- and odd-order Chebyshev filters.

Filter Type and $T(s)$	s-Plane Singularities	Bode Plot for $\lvert T \rvert$	Passive Realization	Op Amp-RC Realization
(a) Low-Pass (LP) $T(s) = \dfrac{a_0}{s + \omega_0}$	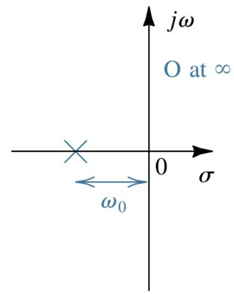	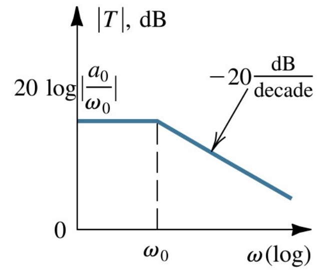	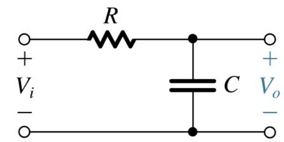 $CR = \dfrac{1}{\omega_0}$ dc gain $= 1$	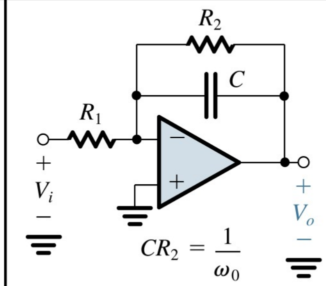 $CR_2 = \dfrac{1}{\omega_0}$ dc gain $= -\dfrac{R_2}{R_1}$
(b) High-Pass (HP) $T(s) = \dfrac{a_1 s}{s + \omega_0}$	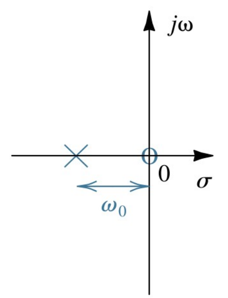	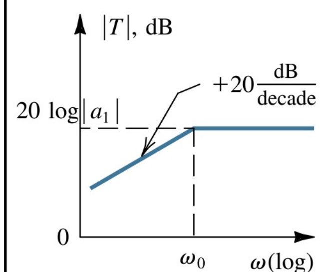	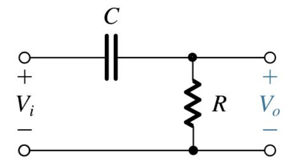 $CR = \dfrac{1}{\omega_0}$ High-frequency gain $= 1$	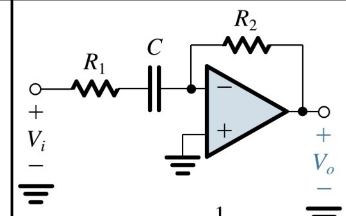 $CR_1 = \dfrac{1}{\omega_0}$ High-frequency gain $= -\dfrac{R_2}{R_1}$
(c) General $T(s) = \dfrac{a_1 s + a_0}{s + \omega_0}$	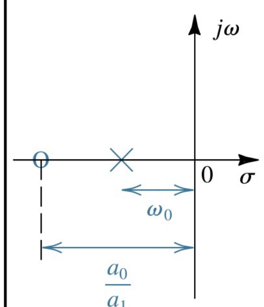	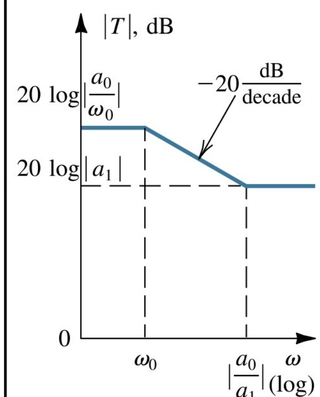	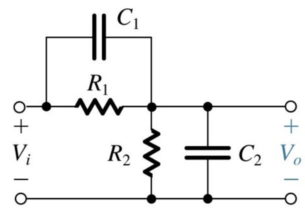 $(C_1 + C_2)(R_1 // R_2) = \dfrac{1}{\omega_0}$ $C_1 R_1 = \dfrac{a_0}{a_1}$ dc gain $= \dfrac{R_2}{R_1 + R_2}$ HF gain $= \dfrac{C_1}{C_1 + C_2}$	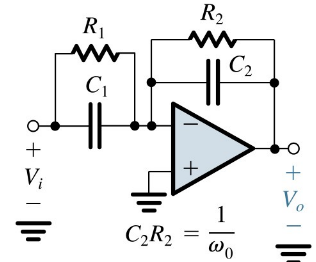 $C_2 R_2 = \dfrac{1}{\omega_0}$ $C_1 R_1 = \dfrac{a_1}{a_0}$ dc gain $= -\dfrac{R_2}{R_1}$ HF gain $= -\dfrac{C_1}{C_2}$

Fig. 11.13 First-order filters.

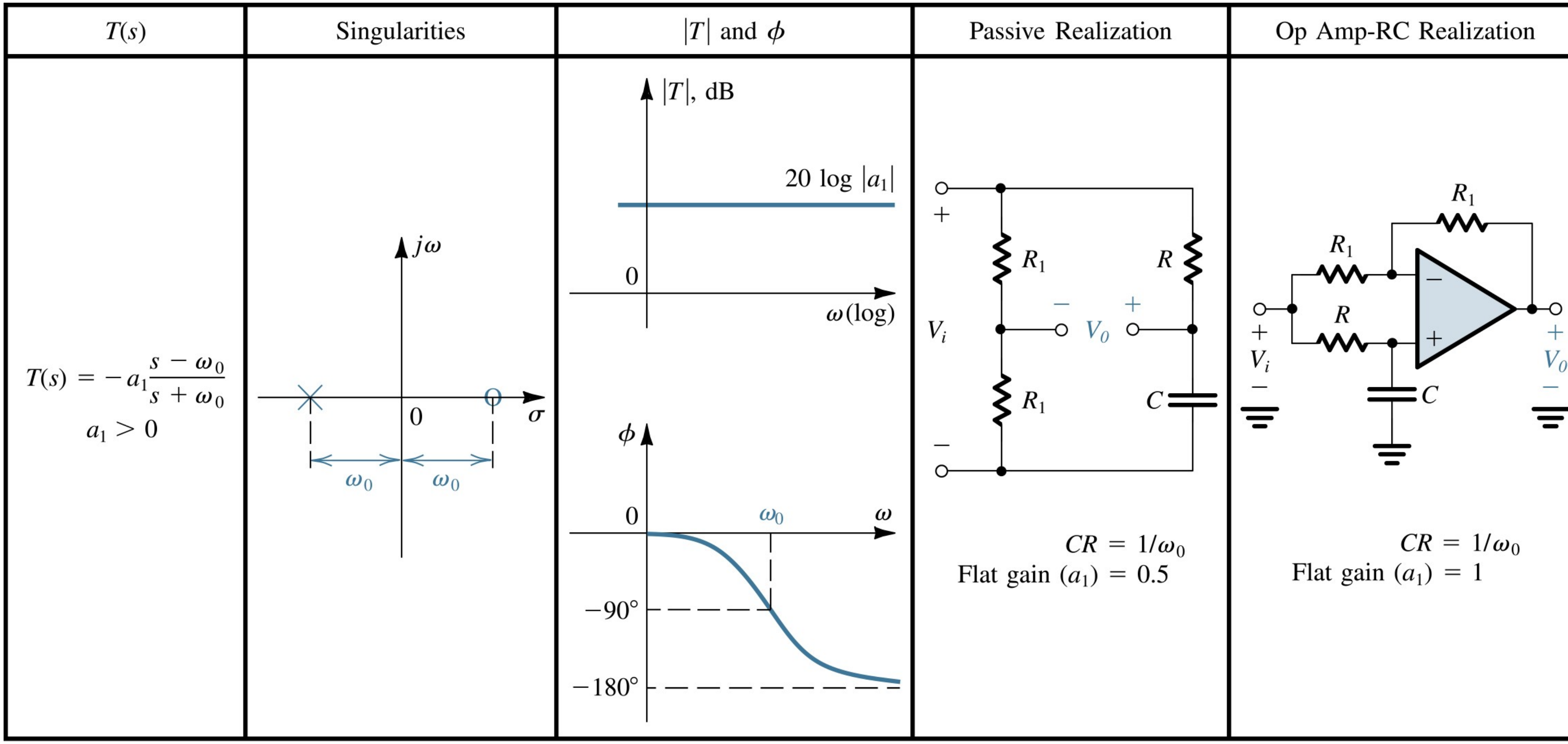

Fig. 11.14 First-order all-pass filter.

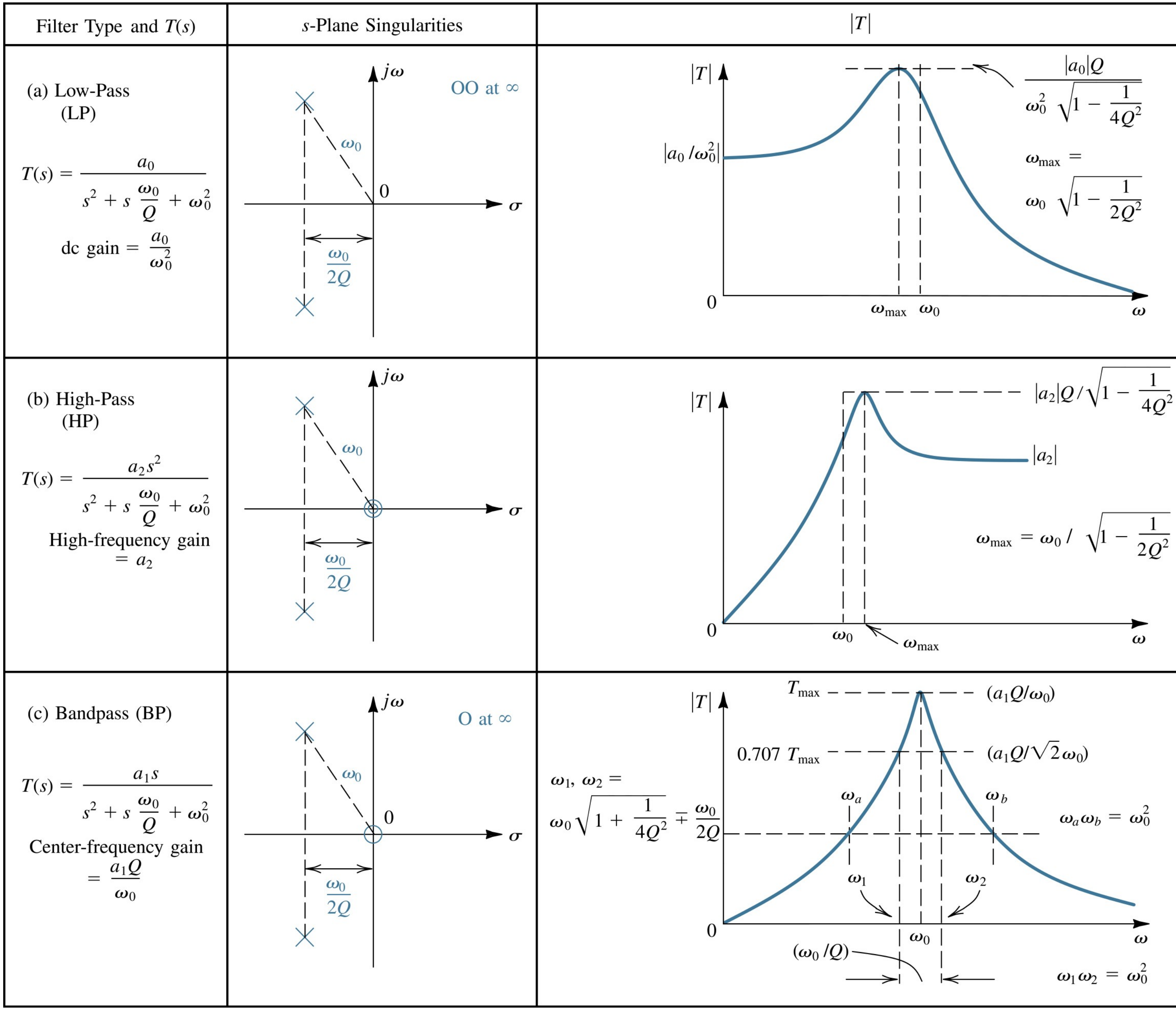

Fig. 11.16 Second-order filtering functions.

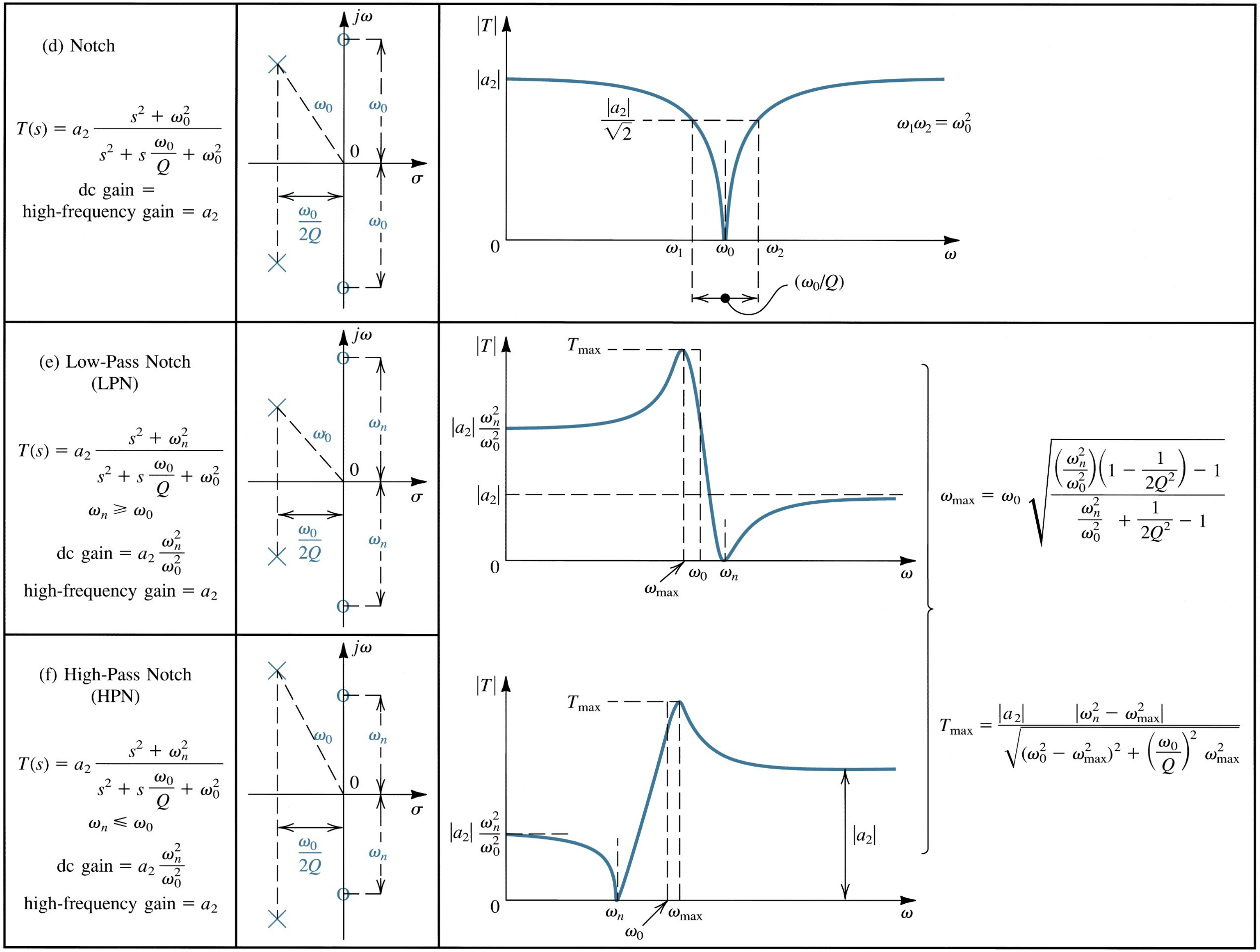

Fig. 11.16 (continued)

(g) All-Pass (AP)

$$T(s) = a_2 \frac{s^2 - s\,\frac{\omega_0}{Q} + \omega_0^2}{s^2 + s\,\frac{\omega_0}{Q} + \omega_0^2}$$

Flat gain $= a_2$

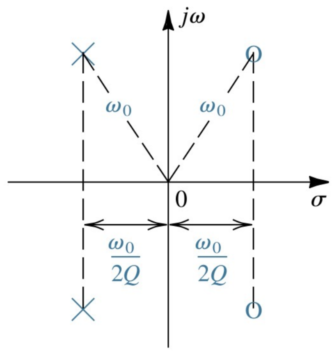

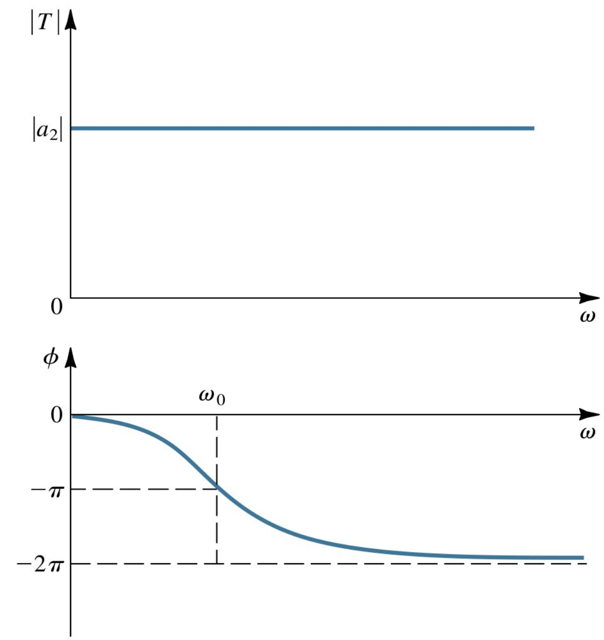

Fig. 11.16 (continued)

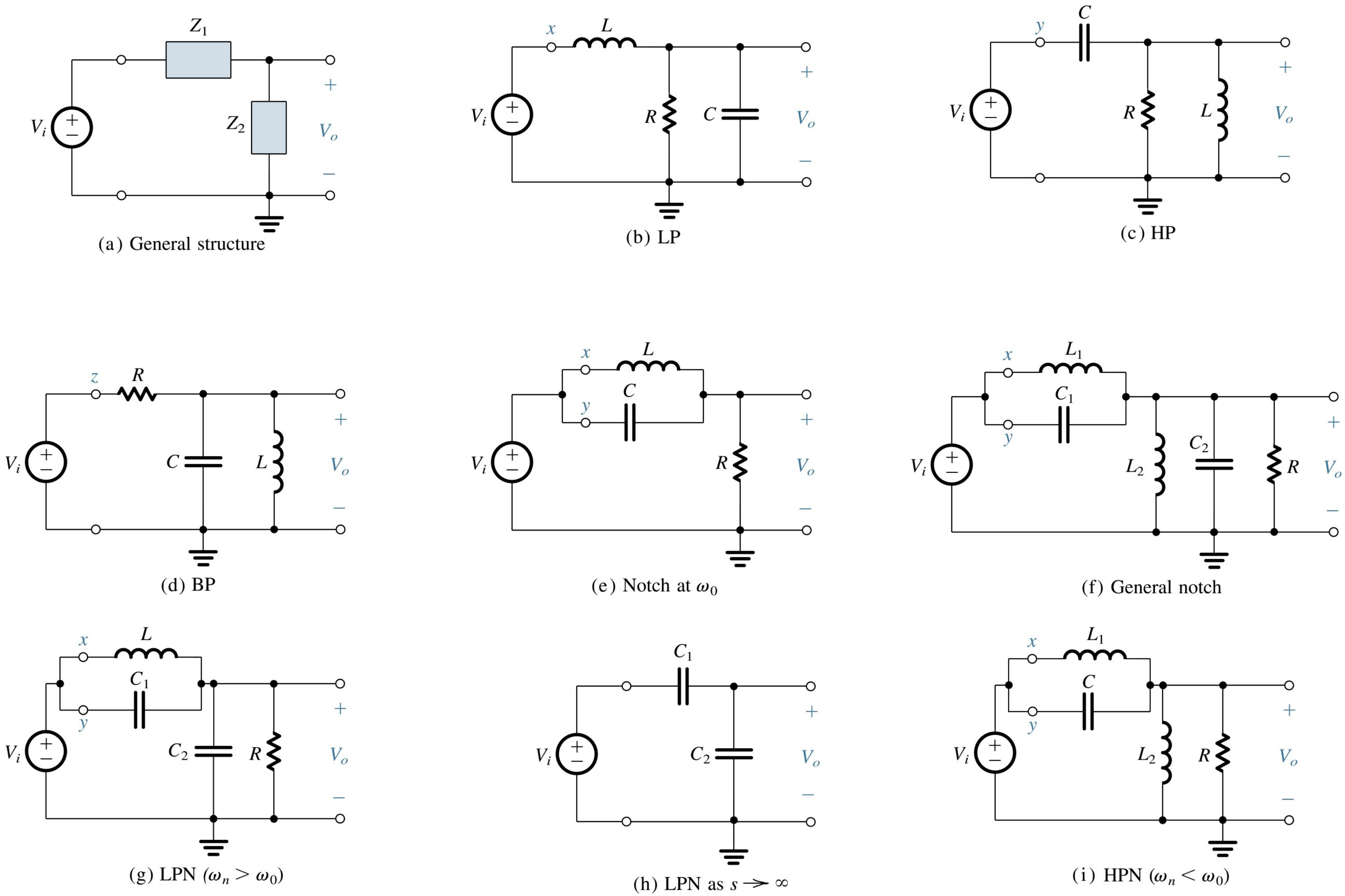

Fig. 11.18 Realization of various second-order filter functions using the LCR resonator of **Fig. 11.17(b)**: **(a)** general structure, **(b)** LP, **(c)** HP, **(d)** BP, **(e)** notch at ω_0, **(f)** general notch, **(g)** LPN $(\omega_n \geq \omega_0)$, **(h)** LPN as $s \to \infty$, **(i)** HPN $(\omega_n < \omega_0)$.

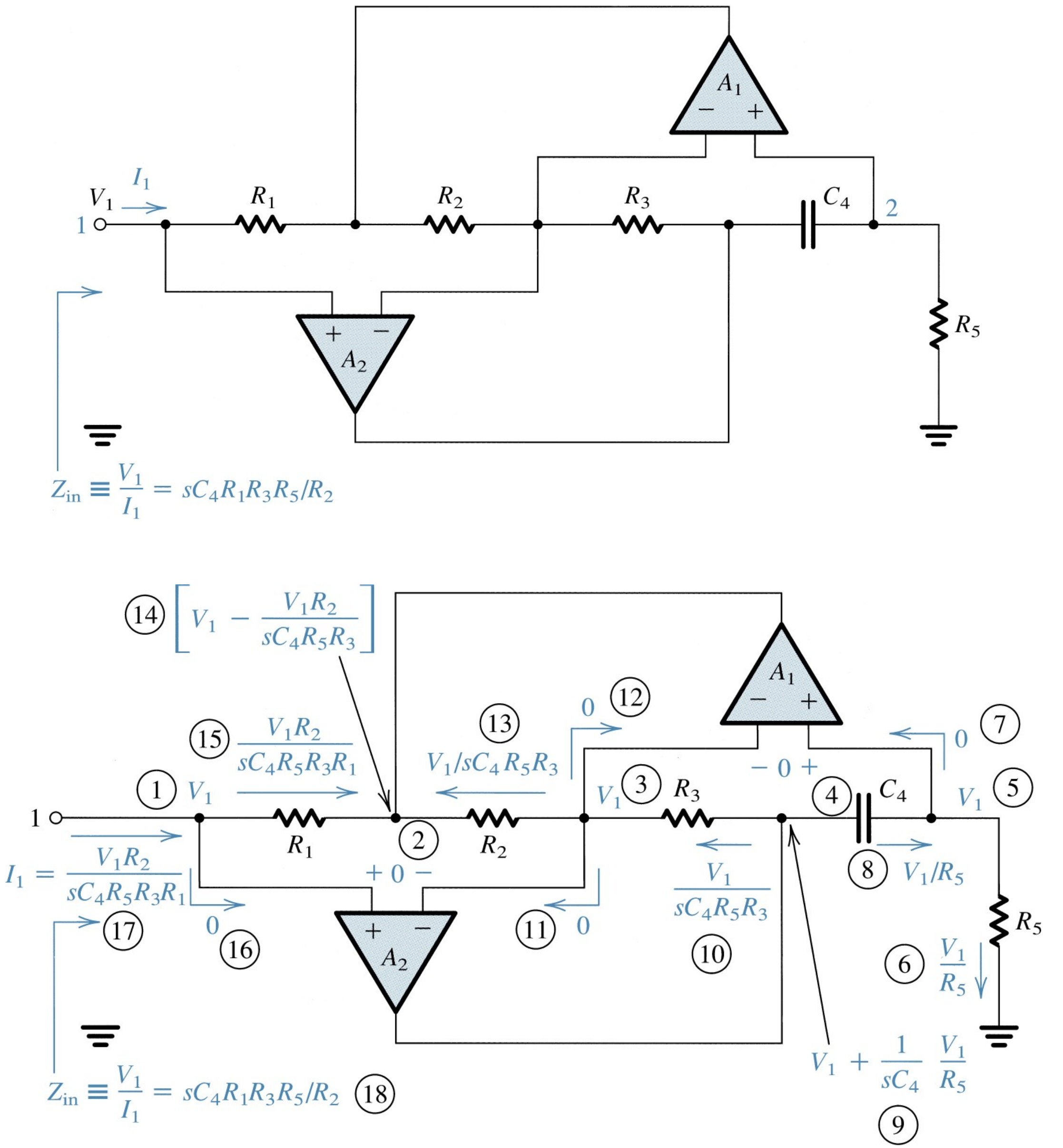

Fig. **11.20 (a)** The Antoniou inductance-simulation circuit. **(b)** Analysis of the circuit assuming ideal op amps. The order of the analysis steps is indicated by the circled numbers.

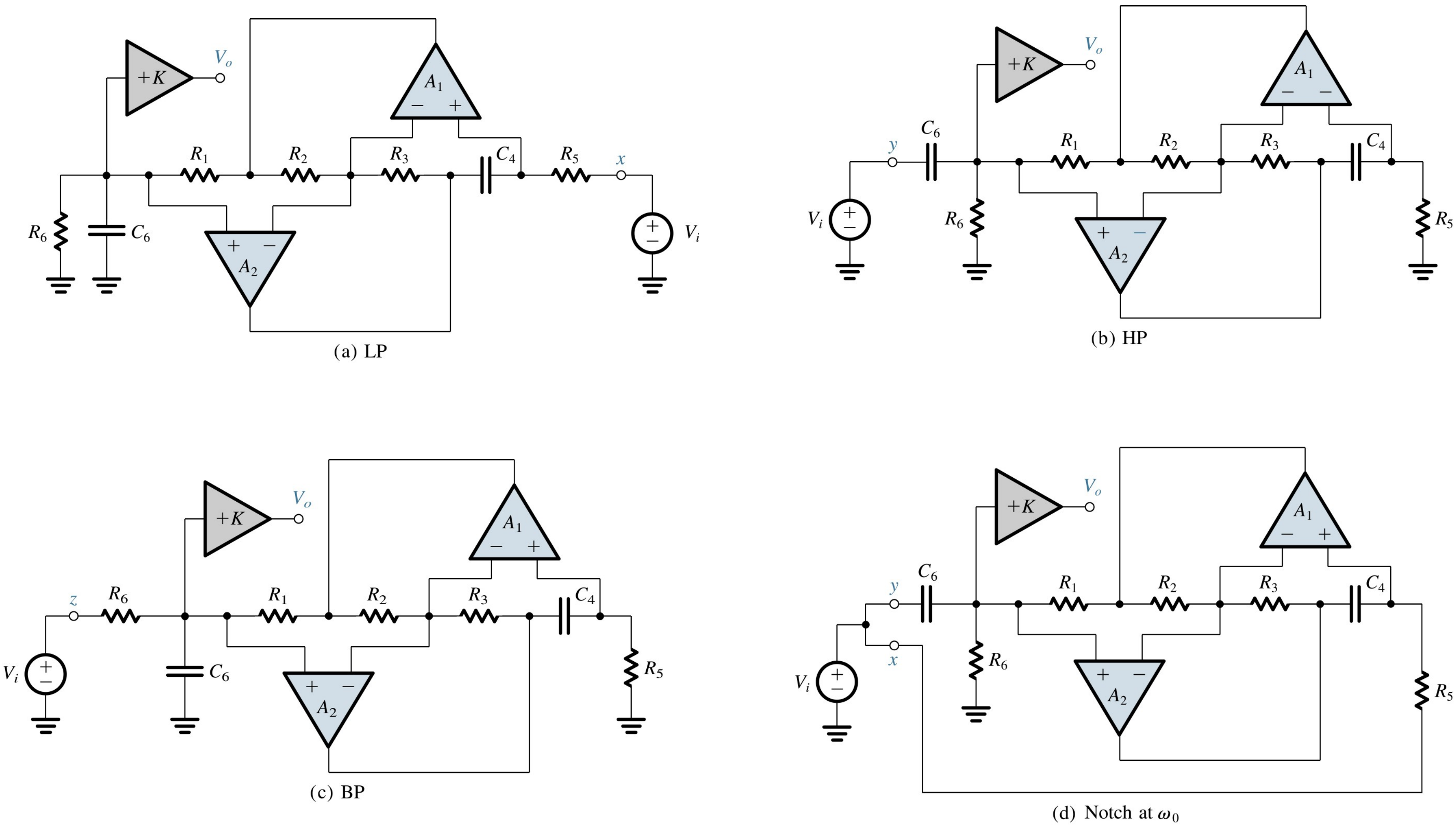

Fig. 11.22a Realizations for the various second-order filter functions using the op amp-RC resonator of **Fig. 11.21 (b)**. **(a)** LP; **(b)** HP; **(c)** BP, **(d)** notch at ω_0;

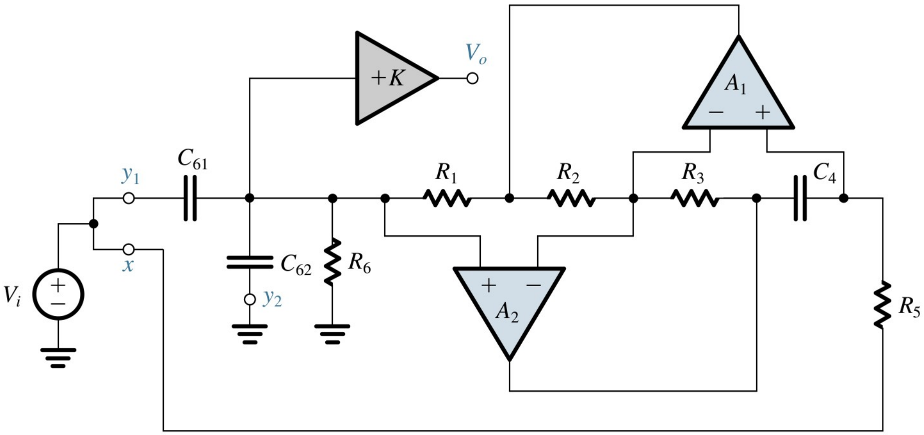

(e) LPN, $\omega_n \geq \omega_0$

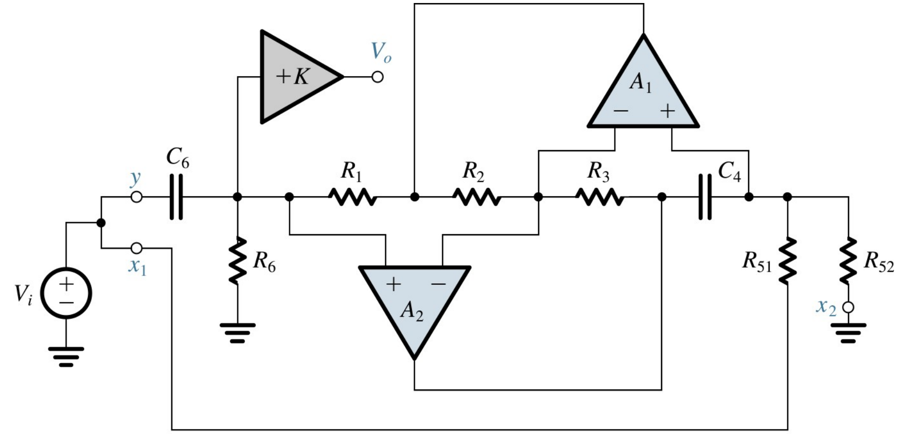

(f) HPN, $\omega_\mathrm{n} \leq \omega_0$

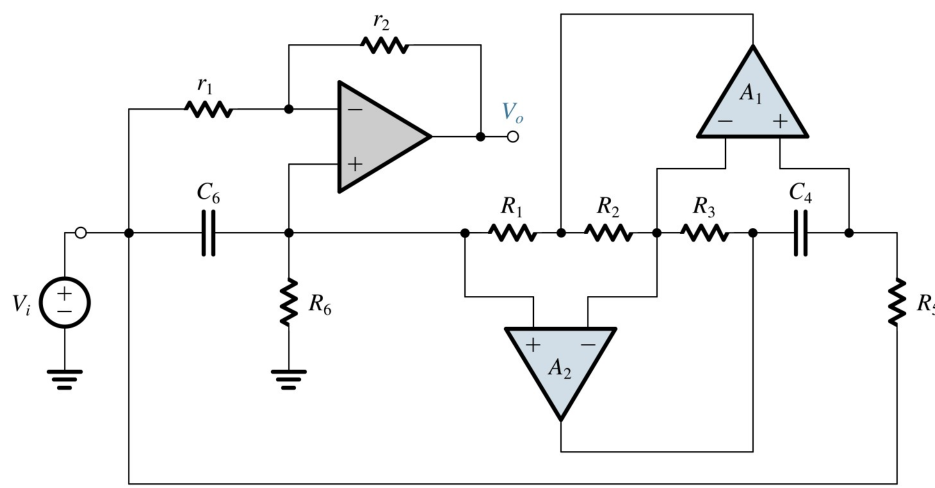

(g) All-pass

Fig. **11.22b** **(e)** LPN, $\omega_n \geq \omega_0$; **(f)** HPN, $\omega_n \geq \omega_0$; **(g)** all-pass. The circuits are based on the LCR circuits in **Fig. 11.18**. Design equations are given in **Table 11.1**.

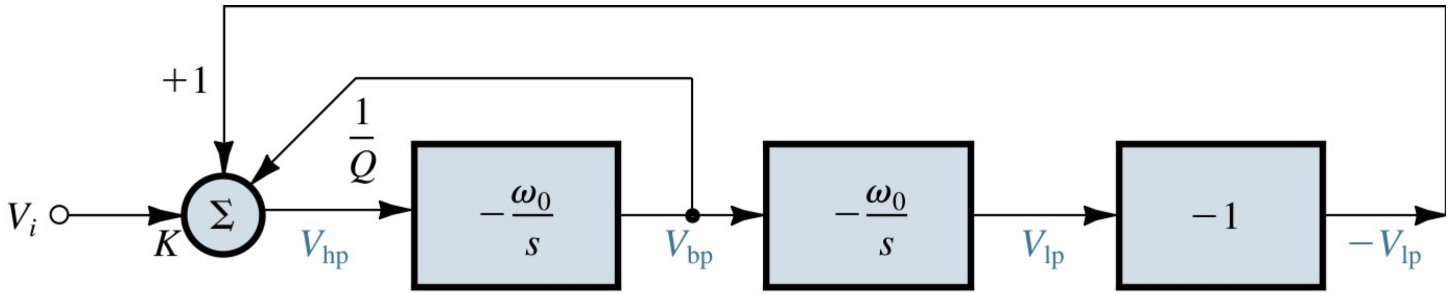

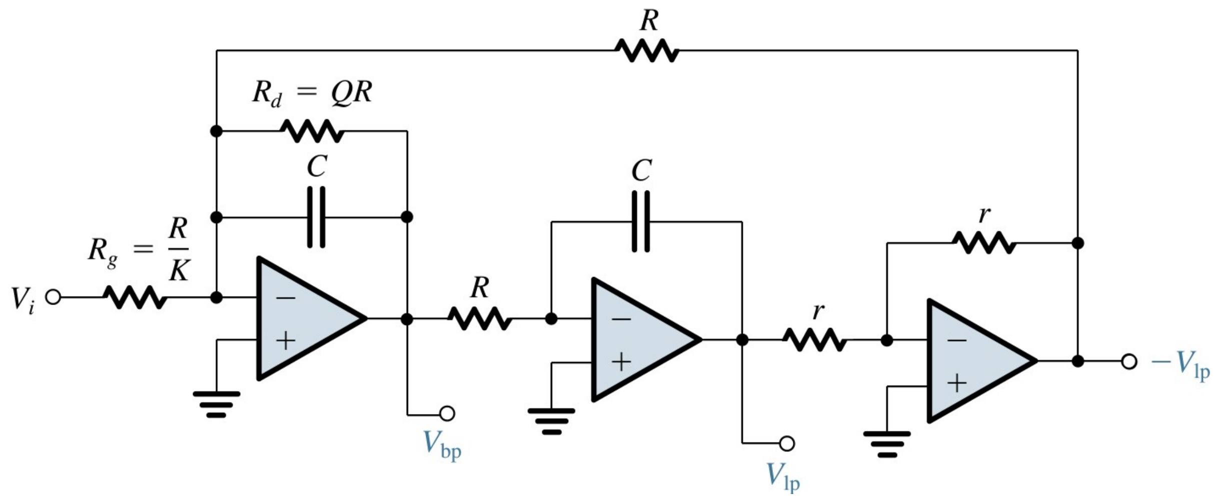

Fig. 11.25 Derivation of an alternative two-integrator-loop biquad in which all op amps are used in a single-ended fashion. The resulting circuit in (b) is known as the Tow-Thomas biquad.

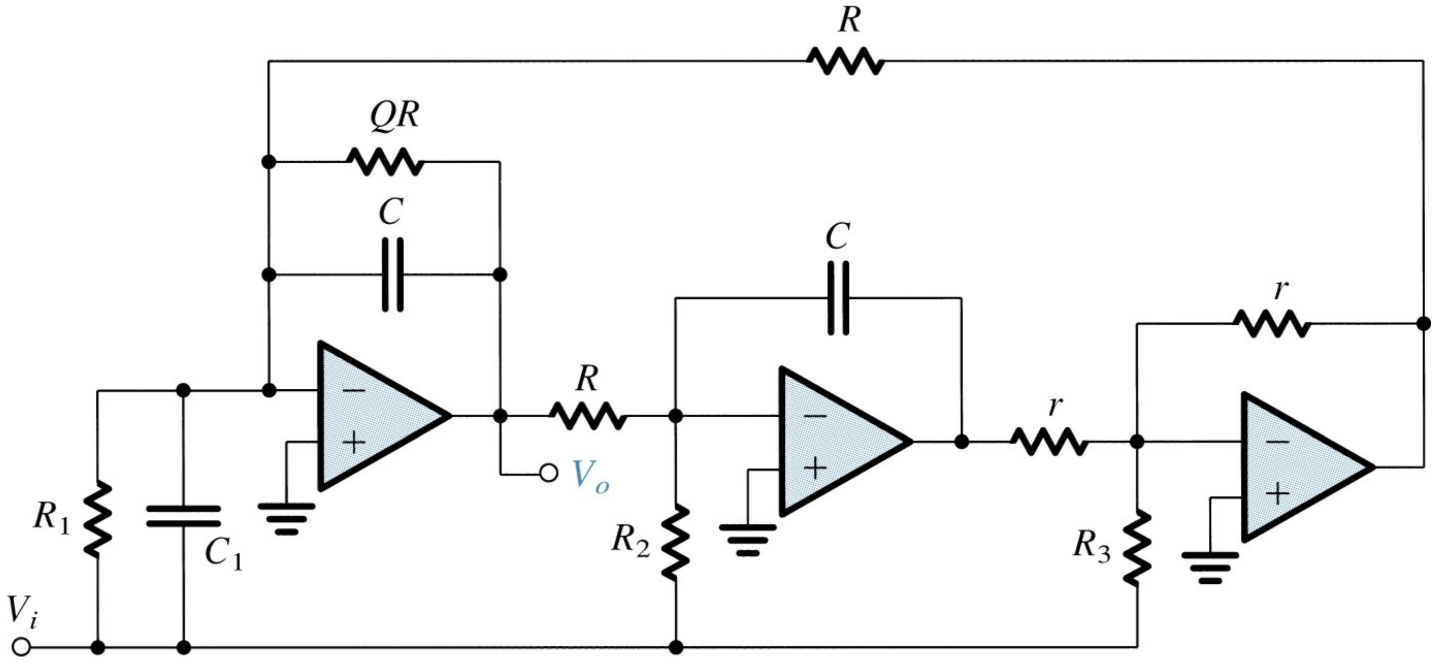

Fig. 11.26 The Tow-Thomas biquad with feedforward. The transfer function of Eq. (11.68) is realized by feeding the input signal through appropriate components to the inputs of the three op amps. This circuit can realize all special second-order functions. The design equations are given in **Table 11.2**.

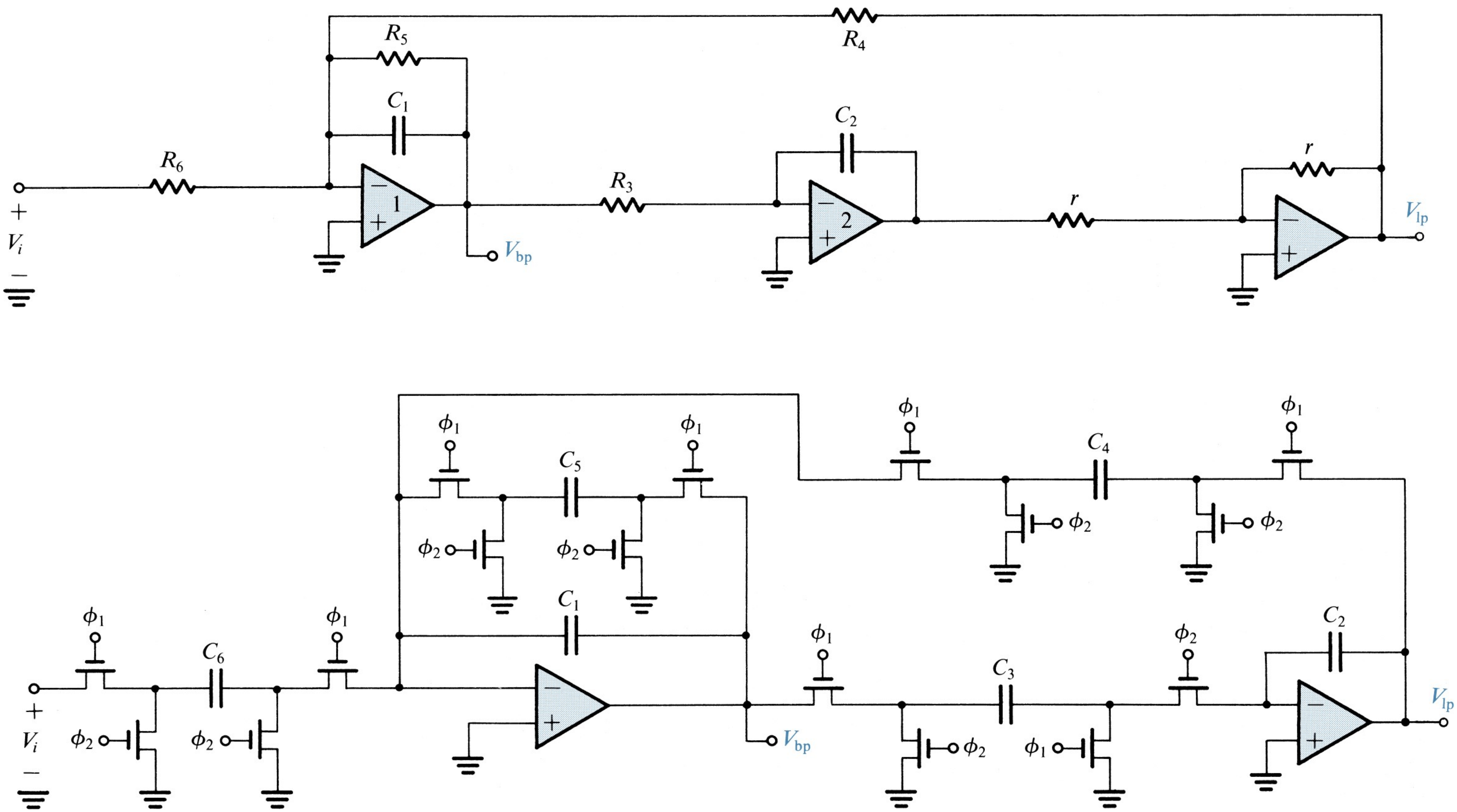

Fig. 11.37 A two-integrator-loop active-RC biquad and its switched-capacitor counterpart.